République Algérienne Democratique et Pobulaire
Ministère De L'enseignement Superieur Et De la Recherche Scientifique
Université Des Frères Mentouri Constantine 1
Facultè Des Sciences de la Tecknologie
Department D'éléctronique

Order N°: ..... **Séries: .....**

Thèse

Présenté pour obtenir le diplome

Doctorat en Télécommunications

Option: Signaux et Systèmes de Télécommunication

THEME

Nouvelles Méthodes pour l'estimation des Paramètres des Distributions Gaussiennes Composées.

Par

BELHI Khadidja

Devant le jury composé de:

Président:	**HAMMOUDI Zoheir**	*Prof.*	**Université des Frères Mentouri Constantine 1**
Rapporteur:	**SOLTANI Faouzi**	*Prof.*	**Université des Frères Mentouri Constantine 1**
Examinateurs:	**MESSALI Zoubeida**	*Prof.*	**Université Bordj Bouarriridj**
	FORTAKI Tarek	*Prof.*	**Université Batna 2**
	BENIERBAH Said	*Prof.*	**Université des Frères Mentouri Constantine 1**

Soutenu le : 27 / 10 / 2022

2022

People's Democratic Republic of Algeria
Ministry of Higher Education and Scientific Research
Frères Mentouri Constantine 1 University
Faculty of Technology Sciences
Department of Electronics

Order N°: ..... Series: .....

A Thesis

Submitted in Partial Fulfillment of the Requirements for

the Degree of Doctorat Troisième Cycle in

Telecommunications

Option: Signals and Telecommunication Systems

THEME

New Methods for Estimating the Parameters of Compound Gaussian Distributions.

By

Khadidja BELHI

Committee Members:

Chairman:	HAMMOUDI Zoheir	*Prof.*	Université des Frères Mentouri Constantine 1
Supervisor:	SOLTANI Faouzi	*Prof.*	Université des Frères Mentouri Constantine 1
Examiners:	MESSALI Zoubeida	*Prof.*	Université Bordj Bouarriridj
	FORTAKI Tarek	*Prof.*	Université Batna 2
	BENIERBAH Said	*Prof.*	Université des Frères Mentouri Constantine 1

2022

Acknowledgment

In the Name of Allah, the Most Gracious and the Most Merciful

First and foremost, all praises to **Allah** for giving me the opportunity, ability, strength, and motivation to accomplish this work.

Second, I would like to sincerely thank my supervisor **Prof. Faouzi SOLTANI** for his guidance, understanding, patience and most importantly, he has provided positive encouragement and a warm spirit to finish this thesis. I have benefited greatly from his extensive knowledge and valuable advice. It has been a great pleasure and honor for me to be under his supervision. I would like to thank and express my special gratitude to **Prof. Amar MEZACHE**, **Dr. Khaireddine Cheikh**, **Dr. Souad CHABBI**, **Dr. Amel AISSAOUI**, **Prof. Atef FARROUKI**, **Prof. Zoheir HAMMOUDI**, **Prof. Toufik LAROUSSI**, and all the teachers who taught me during all my study path, for their valuable advice and support throughout the work period, may **Allah** bless you and give you more success and happiness throughout your life".

I would also like to thank the committee members, **Prof. Zoheir HAMMOUDI**, Frères Mentouri Constantine 1 University, **Prof. Said BENIERBEH**, Frères Mentouri Constantine 1 University, Prof. **Tarek FORTAKI**, Université Batna 2 and **Prof. Zoubida MESSALI**, Université Bordj Bouarriridj, who agreed to be the examiners of this thesis and whose remarks and comments will certainly allow me to improve the quality of this thesis.

Dedications

With Deep Gratitude and Sincere Words,

this thesis is sincerely dedicated to my dear father **"Nachid"**, May God have mercy on him, who has always beensupporting to continue my studies. I hope that work will make him glad and proud of me. Second this thesis is dedicated to my mother **"Saliha DERRAHI"**, who is a struggling woman and who has always been helping me and giving me inspiration and continuously provide their moral, spiritual, emotional, and financial support. Thank you both for giving me the strength to make my dream come true. This thesis is also dedicated to my sisters **"SORIA**" and **"MAROUA"**, my brothers **"Salaheddine"**, **"Memdouh"** and his wife **"Nacera"** and their kids **"Nachid and Aya"** , my dear uncle **"Said"** and my aunt **"Malika"** and my dear cousine **"HADJER"**. Finally, to all the family, friends **"Selma"**, **"Khadidja"**, **"Naziha"**, **"Sara"** and **"Bouchra"** and to all those who are dear to me.

Abstract

RADAR (Radio Detection and Ranging) is a detection system that uses radio waves to determine the distance (ranging) angle or velocity of objects. Two tasks are very important in radar system; Parameters Estimation and Detection of objects. The main task in radar system is to detect an object in homogeneous and non-homogeneous environment. For that, this thesis proposes two contributions which are Parameters Estimation and Detection in Compound Gaussian clutter which accurately describes the behavior of the intensive sea echo "Clutter", in different s ituations. The fi rst co ntribution pr oposed in th is th esis is the estimation of the parameters of the Compound Inverse Gaussian (CIG) distribution which is described by the shape and scale parameters in absence of thermal noise and the results are compared with other estimation methods such as Method of Moments (MoM), Non-Integer Order Moments (NIOM), method of [zlog(z)] and the Maximum Likelihood Estimation (MLE). The proposed method consists of using an iterative procedure the MLE equations using two different methods are used; the MoM which is used as initial points and the MLE which is used to obtain the two equations of the shape and scale parameters for K iterations. After simulations, the results show that the IMLE has the best performance compared with MoM, NIOM, and [zlog(z)] and has similar estimation performance than the MLE method but requires lower computational time. The second contribution concerns the application of the Bayesian Approach to build a CFAR Detector in Pearson V distributed clutter in homogeneous and non-homogeneous environment. The obtained results are compared with Constant False Alarm Rate (CFAR) and its variants as Cell-Averaging CFAR (CA-CFAR), Greatest Ordered CFAR (GO-CFAR), Smallest Ordered CFAR (SO-CFAR) and Ordered Statistic CFAR (OS-CFAR). A new expression of the Probability of False Alarm (pfa) is derived which is different from that of the Neyman-Pearson a pproach. After that we proved that the Bayesian Approach yields a CFAR detector. Then, we use Monte- Carlo method to calculate pd of these detectors. The simulation results show that the Bayesian CFAR detector has the best performance compared with other detectors in different situations even in the presence of high level interferences.

Keywords : CFAR; Clutter; Compound Inverse Gaussian; Pearson V; Bayesian Approach

Résumé

RADAR (Radio Detection and Ranging) est un système de détection qui utilise des ondes radio pour déterminer l'angle de distance (distance) ou la vitesse des objets. Deux tâches sont très importantes dans le système radar ; Estimation des paramètres et détection des objets. La tâche principale du système radar est de détecter un objet dans un environnement homogène et non homogène. Pour cela, cette thèse propose deux contributions qui sont l'Estimation des Paramètres et la Détection dans le Clutter Gaussien Composé qui décrit précisément le comportement de l'écho de mer intensif "Clutter", dans différentes situations. La première contribution proposée dans cette thèse est l'estimation des paramètres de la distribution Compound Inverse Gaussian (CIG) qui est décrite par les paramètres de forme et d'échelle en l'absence de bruit thermique et les résultats sont comparés avec d'autres méthodes d'estimation telles que la méthode des moments. (MoM), les moments d'ordre non entier (NIOM), la méthode de [zlog(z)] et l'estimation du maximum de vraisemblance (MLE). La méthode proposée consiste à utiliser une procédure itérative les équations MLE utilisant deux méthodes différentes sont utilisées ; le MoM qui sert de points initiaux et le MLE qui sert à obtenir les deux équations des paramètres de forme et d'échelle pour K itérations. Après simulations, les résultats montrent que l'IMLE a les meilleures performances par rapport à MoM, NIOM et [zlog(z)] et a des performances d'estimation similaires à celles de la méthode MLE mais nécessite un temps de calcul inférieur. La deuxième contribution concerne l'application de l'approche bayésienne pour construire un détecteur CFAR dans le fouillis distribué Pearson V en environnement homogène et non homogène. Les résultats obtenus sont comparés avec le taux constant de fausses alarmes (CFAR) et ses variantes comme CFAR de moyenne cellulaire (CA-CFAR), CFAR ordonné le plus élevé (GO-CFAR), CFAR ordonné le plus petit (SO-CFAR) et CFAR statistique ordonné (OS -CFAR). Une nouvelle expression de la probabilité de fausse alarme (pfa) est dérivée, différente de celle de l'approche de Neyman-Pearson. Après cela, nous avons prouvé que l'approche bayésienne donne un détecteur CFAR. Ensuite, nous utilisons la méthode de Monte-Carlo pour calculer pd de ces détecteurs. Les résultats de la simulation montrent que le détecteur bayésien CFAR a les meilleures performances par rapport aux autres détecteurs dans différentes situations, même en présence d'interférences de haut niveau.

Mots Clé : TFAC; Fouillis; Gaussian Inverse Composé; Approche Bayésienne

ملخص

RADAR (Radio Detection And Ranging) هو نظام كشف يستخدم موجات الراديو لتحديد زاوية المسافة (المدى) وسرعة الأجسام الثابتة و المتحركة. من المهام الرئيسية لهذا النظام هي تقدير المعلومات و كشف الأجسام .لذلك في هذه الاطرحة تم اقتراح هدفين المتمثلين في تقدير المعلومات و اكتشاف الاجسام في نماذج Compound Gaussian (CG) التي توصف فوضى البحر المكثف (clutter) في مختلف الحالات. الهدف الأول المقترح في هذه الأطروحة هو تقدير معاملات في نموذج (Compound Inverse Gaussian) (CIG) والتي هي معاملات الشكل والمقياس في غياب الضوضاء الحرارية, وقمنا بمقارنتها مع المقدرات الأخرى المتمثلة في طريقة(NIOM)، (MoM)، طريقة [(z) zlog] وتقدير(MLE) . الطريقة المقترحة (IMLE) التي تعتمد على طريقتين مختلفتين هما طريقة اللحظات (MOM) التي يتم استخدامها كنقاط أولية والثاني هو(MLE) الذي يستخدم للحصول على معادلتين من معلمات الشكل والمقياس من اجل K تكرار, حسب النتائج المتحصل عليها نلاحظ ان IMLE لديه أفضل أداء مقارنة ب (NIOM), (MoM), [z log(z)] , ولها أداء تقدير مماثل لطريقة MLE ولكنها تتطلب وقتا حسابيا أقل. الهدف الثاني لهذه الأطروحة يتمثل في بناء كشف Bayesian CFAR في نموذج فوضىPearson V في بيئة متجانسة وغير متجانسة, وقمنا بمقارنتها مع CA-CFAR, SO-CFAR , GO-CFAR و OS-CFAR , استعملنا هذه الطريقة للحصول على معادلة Pfa التي تختلف عن طريقة Neyman-Pearson , ثم استخدمنا طريقة Monte Carlo لحساب Pd هذه الكواشف أظهرت النتائج أن Bayesian CFAR detector لديه احتمالية كشف عالية مقارنة بالكواشف الاخرى في مختلف الحالات حتى لوأضفنا مستوى عالي من الفوضى الشائكة و التداخلات.

كلمات مفتاحية: ضوضاء، التداخلات، الكواشف، نهج بايزي، مركب معكوس غاوسي

Contents

List of Abbreviations

CFAR	Constant False Alarm Rate
CNR	Clutter-to-Noise Ratio
CUT	Cell Under Test
CIG	Compound Inverse Gaussian
CG	Compound Gaussian
CA-CFAR	Cell-Averaging CFAR
CW	Continuous Wave
GO-CFAR	Greatest-Of CFAR
HF	High Frequency Hertz
IF	Intermediate Frequency
IID	Identically and Independent Distributed
IRF	Inter Pulse Frequency
MSE	Mean Square Error
MLE	Maximum Likelihood Estimate
$G\Gamma$	Generalized gamma
MTI	Moving Target Indicator
MIMO	Multiple Input Multiple Output
NP	Neyman Pearson
OS-CFAR	Order Statistics CFAR
PDF	Probability Density Function
Pfa	Probability of False Alarm
Pd	Probability of Detection
PRF	Pulse Repetition Frequency
Pr	Probabilty

PSR	Primary Surveillance Radar
PRF	Pulse Repetition Frequency
RADAR	RAdio Detection And Ranging
RCS	Radar Cross Section
SNR	Signal to Noise Ratio
GSNR	Generalized SNR
ICR	interference-to-Clutter Ratio
SO-CFAR	Smallest-Of CFAR
SSR	Secondary Surveillance Radar
SAR	Synthetic Aperture Radar
T/R	Transmitter/Receiver
UHF	Ultra High Frequency
VHF	Very High Frequency

List of Symbols

Chapter 2

R	Range
C	Speed of light
σ	Target cross section
E_i	The incident electric field strength at target
P_t	Transmitted power
$\hat{P}'$	Power density
P_r	Received Power
G	Antenna gain
R_{max}	Maximum radar range
A_e	Antenna effective aperture
τ	Pulse width
σ^0	Area reflectivity

Chapter 3 and 4

K_ν(X)	Modified Bessel function
μ	Mean power of the inverse Gaussian distribution
λ	Shape parameter of the inverse Gaussian distribution
$\hat{.}$	Estimated parameter
a	Scale parameter of Weibull distribution
b	Shape parameter of Weibull distribution
α	Shape parameter of Pareto distribution
β	Scale parameter of Pareto distribution
b	Scale parameter of the K-distribution
m_1, m_2	First and second order moments of inverse Gaussian distribution
H_0, H_1	Binary Hypothesis
T	Detection threshold
Pfa	Probability of False Alarm
Pd	Probability of Detection

List of Figures

List of Tables

Chapter 1

General Introduction

Contents

Abstract

This chapter is introductory and informative; it contains a historical overview of radar systems and its importance in maritime and coastal surveillance. It also includes the main motivation and problems addressed in this thesis. Finally, it supplies a plan of this thesis.

1.1 Introduction

Our reaserch work is mainly based on system which is RADAR. We start this thesis by giving general ideas about this topic. RADAR is (Radio Detection and Ranging) a detection system that uses radio waves to determine the distance (ranging) angle or velocity of objects. A RADAR system consists of a transmitter producing electromagnetic waves and a receiver which receives reflected radio waves from objects present in the surveillance space and giving information about the objects location and speed.
Serious developmental work on radar began in the 1930s, but the basic idea of radar had its origins in the classical experiments on electromagnetic radiation conducted by German physicist Heinrich Hertz during the late 1880s. Maxwell had formulated the general equations of the electromagnetic field, determining that both light and radio waves are examples of electromagnetic waves governed by the same fundamental laws but having widely different frequencies. Maxwell's work led to the conclusion that radio waves can be reflected from physical objects called targets. The theory and radar technology were developed during the Second World War [1]. After the war, progress in radar technology slowed considerably. New and better radar systems emerged during the 1950s where radar has found wide-ranging civilian applications since these years, including air traffic control, meteorology, road monitoring, and measuring swarms of insects. So, radar technology has been improved by several researchers who worked in this domain, the basic technology doesn't change but the systems of object detection has been improved by several methods. In radar systems, the most important tasks are modelization, estimation and detection. One of the most important problems in radar systems is automatic target detection. In practical radar signal detection systems, the problem is to automatically detect a target in a nonstationary noise and clutter bacckground while maintaining a constant of false-alarm. Clutter is the term applied to any unwanted radar signal from scatterers that are not of interest to the radar user. Examples of unwanted signals, or clutter, in radar signal detection are reflection from terrains, sea, rain, birds, insects,etc. Several methods were proposed to analyze radar detection. These methods are called constant false alarm rate (CFAR) detectors [2, 3, 4]. In radar systems, before detection step there's another important step which consists of estimating the parameters of the clutter distribution. A lot of methods were proposed to estimate the parameters of clutter distributions in homogeneous and non homogeneous clutter. In practical situations, the environment isn't homogeneous. This non homogeneity is caused by a clutter edge or the presence of interferences , and we always use these two situations to check the robustness of the detection algorithm. In this thesis, we propose methods for estimation and detection to improve the detection performance of objects especially in spiky clutters.

1.2 Motivations and Contributions

RADAR sensors are a powerful tool for detecting targets in the maritime environment. The compound Gaussian models where originally proposed for modeling sea clutter by ward [5] such as compound inverse Gaussian ,etc. While there are three problems looking to analyse in RADAR technology which are modelization, estimation and detection. Our work is based on two problems that are estimation and detection. Several methods have been proposed to estimate the parameters of compound Gaussian clutter such as MLE,[zlog(z)],NIOM and MoM [6, 7, 8]. The MLE has always the best performance compared with the others but it requires higher computational time. So the first problem is to propose an iterative method to derive the parameter estimation of the MLE method in order to reduce the computational time. The appearance of non-Gaussian models led to new theoretical problems that complicate the detection task and must be resolved. CFAR detection methods (CA-CFAR, SO-CFAR, GO-CFAR, OS-CFAR ect) were proposed by [2, 3, 4] to resolve these problems. When the clutter becomes spiky, the detection in the tail region becomes complicated . For this, we applied the Bayesian appraoch to built a detector for a clutter obeying to the Pearson V distribution. The proposed contributions of this thesis are mainly based on the following points:

1.2.1 Iterative Maximum Likelihood Estimation

The first contribution in this work concerns the estimation parameters of Compound Inverse Gaussian distributed clutter under the assumption of the absence of thermal noise, which is considered as compounds distribution with speckle and texture. We used Iterative Maximum Likelihood estimation (IMLE) method to estimate the scale and shape parameters of this distribution. This method is based on two different methods: method of MoM and MLE. The IMLE method is compared with other exsiting methods in the literature [9] such as MLE, NIOM, HOME and [zlog(z)]. We simulated all these estimators and the results obtained show that the IMLE method outperforms all the other methods and has similar estimation performance than the MLE method but requires lower computational time.

1.2.2 Bayesian approach detector

In the second contribution, we propose to use the Bayesian approach as a detector for a clutter following the Pearson V distribution in homogeneous and non homogeneous environement. The no homogeneity is modeled as a step function discontinuity in the reference window, this method is used to construct the Bayesian predictive distribution of the cell under test (cut) giving the reference cells. First we derived the expression of the Pfa using this method then the Pd was calculated by Monte Carlo simulation and the obtained results were compared with CFAR detectors which were discssued in [10]. The results showed that the Bayesian detector has better performance than CFAR detectors in homogeneous and non homogeneous clutter.

1.3 Thesis Organization

Given the importance of the presentation of this thesis, we have structured this manuscript around five chapters:

Chapter 2 presents some of the radar concepts, such as their operation, classifications and applications. This chapter also provides an overview of estimation and detection methods.

Chapter 3 presents the estimation of the two parameters of the CIG distribution using IMLE method. This chapter is also contains genral ideas about different distributions and estimation methods. The simulation is compared with other estimators.

Chapter 4 presents the Bayesian approach detector in homogeneous and non homogeneous clutter modeled by Pearson type V. In this chapter, we derive the expression of Pfa. The simulation of Pfa and Pd are compared with others (CFAR) detector.

Chapter 5 presents the main conclusions. Also, this chapter lists the possible views and suggestions that could serve as an extension of the work proposed in this thesis.

Chapter 2

Radar Concept

Contents

Abstract

This chapter provides the necessary information that helps to understand the proposed work in the following chapters. For more details, the interested reader is invited to review the general literature on radar systems such as [11, 13, 14].

2.1 Radar Basics

A radar is an electromagnetic sensor used for detecting, locating, tracking and recognizing objects of various kinds at considerable distances. It operates by transmitting radio frequency electromagnetic waves toward objects, commonly referred to as targets, and observing the echoes returned from them. The targets may be aircraft, ships, spacecraft, automotive vehicles, and astronomical bodies, or even birds, insects, and rain. Figure 2.1 shows the different elements involved in the processes (transmission, propagation through the atmosphere and reflection from the target) constituting a mono static radar signal [11, 12]. Although the details of a radar system vary, the main subsystems include a transmitter, antenna, receiver, and signal processor. The electromagnetic waves are generated by the transmitter, the principal role of antenna is that takes these waves from the transmitter and introduces them into the atmosphere. The transmitter is connected to the antenna through a device which is usually a switch or a circulator known as transmit/receive (T/R) device. The function of this device is a connection point that the transmitter and the receiver can both be attached to the antenna simultaneously. at the same time it protects the sensitive receiver components from the high powered transmit signal because it is used as isolation between the transmitter and receiver. The transmitted wave propagates toward the environment to the target that it induces currents on the target (surface). Other surfaces on the ground and in the atmosphere reradiate the signal. These unintentional and unwanted reflections are called clutter. The electromagnetic waves are reflected from an object and are received by the radar receive antenna. So, the receiving antenna receives a portion of the reflected waves from an object. This object may be a target of interest or may be of no interest such as clutter. The reception circuits amplify and convert the radio frequency signal to an intermediate frequency (IF), then the signal is fed into the detector to remove the carrier wave from the modulated signal, and then apply the signal to an analog-to-digital converter. The signal processor extracts the required information, such as the presence, absence, speed and range of the target [12].

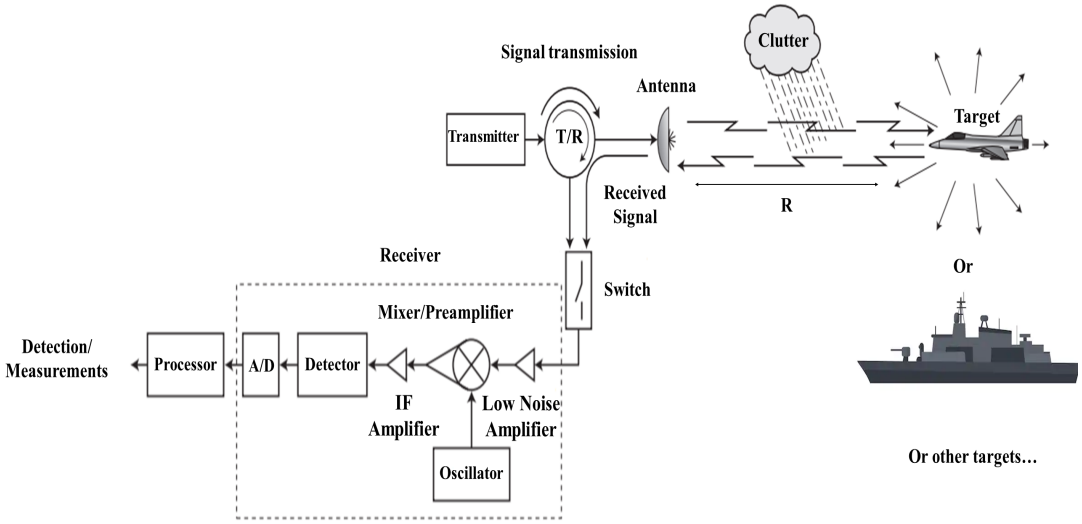

Figure 2.1: The radar concepts.

2.2 Basic elements of a radar system

In a radar system, there are five elements which are: a transmitter, a duplexer, an antenna, a receiver and an indicator. Figure 2.2 shows the configuration of these elements with some associated elements. The function of these principal elements is described in [13].

- **Transmitter**: This device is one of the major elements in radar system. It generates the radio frequency (RF) power signal to illuminate the target.
- **Duplexer**: The duplexer alternately switches the antenna between the transmitter and receiver so, that only one antenna is used. This switching is necessary because the high-power pulses of the transmitter would destroy the receiver if energy is allowed to enter the receiver.
- **Antenna**: The Antenna transfers the transmitter energy to signals in space with the required distribution and efficiency. This process is applied in an identical way on reception.
- **Receiver**: The receivers amplify and demodulate the received RF-signals. The receiver provides video signals on the output.
- **Indicator**: The indicator should present to the observer a continuous, easily understandable, graphic picture of the relative position of radar.

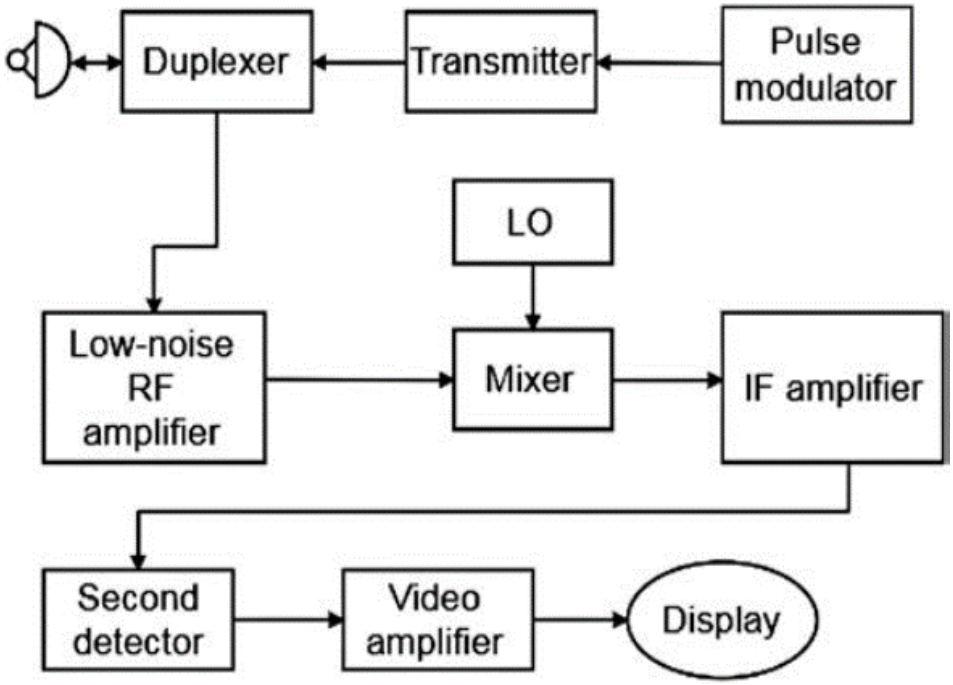

Figure 2.2: block diagram of primary radar.

2.3 Information available from the radar echo

Although the name radar is derived from radio and detection, it is capable of providing more information about the target than is implied by its name. The detection of the target denotes figuring out of its presence. Detection is considered independently of the process of information extraction, but it is not often that we are interested in knowing only that the target is present without knowing something about its location in space and its nature. For that, in radar system the extraction of useful information is an important of radar operation. Information extraction generally requires matched filters for optimum processing. The more information that is known about the target a priori, the more efficient will be the detection. For example, if the target location is known, the antenna can be pointed in the correct direction, energy and time need not be wasted searching empty space. Or, if the relative velocity is known, the receiver can set the correct reception frequency, negating the need to search the frequency band over which the Doppler shift might occur. The rate of change of target location can also be measured from the change in range and angle with time, from which the track can be established. In many radar applications, detection is not said to occur until its track has been established. A radar with sufficient resolution in one or more coordinates can determine a target's size and shape. Polarization allows a measure of the symmetry of a target. In principle, a radar can also measure the surface roughness of a target and determine something about its dielectric properties [11].

2.3.1 Range

The ability to set range by measuring the time for the radar signal to propagate to the target and back is probably the distinguishing and most important characteristic of conventional radar. No other sensor can measure range to the accuracy of a radar, at such long ranges, and under adverse weather conditions. Radar has demonstrated its ability to measure interplanetary distances to an accuracy limited only by the accuracy to which the velocity of propagation is known. At more modest distances, the measurement of range can be made with a precision of a few centimeters. The usual radar waveform for determining range is the short pulse. The shorter the pulse, the more precise can be the range measurement. A short pulse has a wide spectral width (bandwidth). A CW waveform with frequency or phase modulation can also provide an accurate range measurement. It is also possible to measure the range of a single target by comparing the phase difference between two or more CW frequencies. Range measurement with CW waveforms has been widely employed, as is case the radar altimeters and aircraft scanners [11]. The range R of the target is obtained by measuring the time delay Δt taken by the pulse to travel a two-way path between the radar and the target. Since the electromagnetic energy propagates at the speed of light $c = 3 \times 10^8 m/sec$, in free space, the range, R, is

$$R = \frac{c\Delta t}{2} \tag{2.1}$$

Where, R is in meters and Δt is in seconds.

2.3.2 Radial velocity

From successive measurements of range the rate of change of range, or radial velocity, can be obtained. The Doppler frequency shift of the echo signal from a moving target also provides a measure of radial velocity. However, the measurement of Doppler frequency in many pulse radars is highly ambiguous, reducing its utility as a direct measurement of radial velocity. When it can be used, it is often preferred to successive range measurements since it can achieve a more accurate measurement in a shorter time. Any measurement of velocity, whether by the rate of change of range or by the Doppler frequency shift, requires time. The longer the time of observation, the more accurate can be the measurement of velocity. A longer observation time also can increase the signal-to-noise ratio, another factor that results in increased accuracy. Although Doppler frequency shift is used in some applications to measure radial speeds, such as police speedometer and satellite surveillance, it is widely used as the basis for sorting out moving targets from unwanted echoes, as in MTI and AMTI (Airborne MTI) and CW radars [11].

2.3.3 Angular direction

The direction of a target is determined by sensing the angle at which the returning wave front arrives at the radar. This is achieved usually by using a directional antenna, with a narrow beam. The direction in which the antenna points when the received signal is a maximum indicates the direction of the target. As well as other methods for measuring angle, assumes that the atmosphere does not perturb the straight-line propagation of the electromagnetic waves. The direction of the incident waveform can also be determined by measuring the phase difference between two separated receiving antennas, the accuracy of the angle of arrival depends on the extent of the antenna aperture. The wider the antenna, the narrower the beam-width and the better the accuracy. The determination of angle basically involves only the one-way path. Nevertheless, the angle measurement is an integral part of most surveillance and tracking radars.

2.3.4 Radar Cross Section (RCS)

The radar range equation expresses the range at which a target may be detected with a given probability by a radar having a given set of parameters. This equation includes the radar cross section (RCS) of an equivalent isotropic radiator, an important parameter that defines the scattering efficiency of a target. The RCS is essential in the calculations of radar range and the SNR. The target's RCS may be viewed as a comparison of the strength of the reflected signal from a target to the reflected signal from a perfectly smooth sphere of cross-sectional area of $1m^2$. In fact, the RCS is defined as an equivalent cross-section of the target producing the same amount of energy returned to the radar as would be produced by an isotropic radiator. The RCS and the actual area of the target are, therefore, not directly related through some simple equation [13]. The RCS of a target is a measure of its ability to reflect electromagnetic energy in the direction of the radar receiver, and its value is expressed as an area. This reflected energy is dependent on a multitude of parameters such as: the radar transmitters frequency, the direction of the illuminating radar, target geometry, The material of which the target is made, the absolute size of the target, the incident angle (angle at which the radar beam hits a particular portion of the target which depends upon the shape of the target and its orientation to the radar source), the polarization of the transmitted and the received radiation with respect to the orientation of the target [13].The RCS, denoted by the symbol σ, is the area intercepting that amount of power which, when scattered equally in all directions, produces an echo signal at the radar equal to that from the target. In other terms [11]:

$$\sigma = \frac{\text{power reflected back to receiver per unit solid angle}}{\text{(incident power density intercepted by the target)}/4\pi} = \lim_{R \to +\infty} 4\pi R^2 \left| \frac{E_r}{E_i} \right|^2 \tag{2.2}$$

Where R is the distance between the radar and target, E_r is the reflected electric field strength at radar, and E_i is the incident electric field strength at target.

2.4 Radar Equations

The radar equation relates the range of a radar to the characteristics of the transmitter, receiver, antenna, target, and environment. It is useful to determine the maximum distance of the target from the radar. It can also serve both as a tool for understanding radar operation and as a basis for radar system analysis and design. This section provides a simple form of radar equation. If the power of the radar transmitter is denoted by P_t, and if an isotropic antenna is used, which radiates the same electromagnetic energy in all directions. The power density $\hat{P}'_t$ at a distance R from the radar is equal to the transmitter power divided by the surface area $4\pi R^2$ of an imaginary sphere of radius R. This expressed as [11]:

$$\hat{P}'_t = \frac{P_t}{4\pi R^2} \tag{2.3}$$

Radar systems use directional antennas instead of isotropic antennas to concentrate the power density in a certain desired direction. The Gain G of an antenna is the radiation intensity of the antenna in a given direction over that of an isotropic antenna By definition, the gain of a directional antenna is the ratio of the intensity in the direction of maximum radiation to the radiation intensity from a lossless, isotropic antenna, both measured at a constant range with the same power input. The power density at the target at a distance R from the radar using a directive antenna with a transmitting gain G is then expressed as

$$\hat{P}_t = \frac{P_t G}{4\pi R^2} \tag{2.4}$$

The target intercepts the electromagnetic wave, and as results, the incident energy will be scattered in various directions, the measure of the amount of incident energy that a radar target intercepts and scatters back toward the radar is denoted as Radar cross section σ which is expressed in section (2.3.4). The RCS describes the ability of the target to scatter the incident energy, and is defined as 4π times the ratio of the power per unit solid angle reflected by the target in the direction of the radar to the power density of the incident wave at the target. the RCS is given as:

$$\sigma = 4\pi R^2 \frac{P_b}{P_t} \tag{2.5}$$

Where P_b is the power per unit solid angle reflected back in the direction of the radar. Thus the total reflected power by the target is

$$P = \frac{P_t G \sigma}{4\pi R^2} \tag{2.6}$$

Considering the reflected power as a uniform source of power located at the target, the power density $\hat{P}$ of the energy at the radar can be expressed as

$$\hat{P}_t = \frac{P_t G}{4\pi R^2} \frac{\sigma}{4\pi R^2} \tag{2.7}$$

The radar antenna captures a portion of the returned echo. Assuming that the area capturing this energy is equal to the effective area of the receiving antenna A_e, the total power received by the radar is then given by:

$$P_r = \frac{P_t G A_e \sigma}{(4\pi R^2)^2} \tag{2.8}$$

If the echo signal is having the power less than the power of the minimum detectable signal, then Radar cannot detect the target since it is beyond the maximum limit of the Radar's range. Therefore, we can say that the range of the target is said to be maximum range when the received echo signal is having the power equal to that of minimum detectable signal S_{min}. The simple form of the radar equation becomes:

$$R_{max}^4 = \frac{P_t G A_e^2 \sigma}{(4\pi)^2 S_{min}} \tag{2.9}$$

The important antenna parameters are the transmitting gain and the receiving effective area. Antenna theory gives the relationship between the transmitting gain and the receiving effective area of an antenna as:

$$G = \frac{4\pi A_e}{(\lambda)^2} \tag{2.10}$$

Where λ is the wavelength. In general radar systems uses the same antenna for both transmission and reception. So, Equation (1.10) can be substituted into Equation (1.9), to give other form of the radar equation:

$$R_{max} = \left[\frac{P_t A_e^2 \sigma}{4\pi \lambda^2 S_{min}} \right]^{1/4} \tag{2.11}$$

This is the basic form of some of the radar equations. Which are published with more details in [11, 12, 13].

2.5 Types of radar systems

Radar technology is one of the most advanced technologies for measuring object distances, because of this, there has been a variety of radar systems that are used for various purposes. Radar systems are classified under various categories depending on the functions and purposes such as mission of the radar, antenna type, frequency band, the specific measurements it is to make, the wave-forms it utilizes, the physical environment in which it must operate etc.

Some of the most common radar systems employed under different functions and used by different sectors.

2.5.1 Primary and secondary radar

Primary Surveillance Radar (PSR) transmits electromagnetic signal energy towards the target and the receiver receives the returned echo to extract information. The target acts as passive element and reflects the EM energy back towards the primary radar antenna. The relationship between the echo strength and the range presents a major problem for long-range detection. It is also very difficult to determine the altitude of an aircraft accurately using primary radars. Secondary Surveillance Radar (SSR) transmits EM signal energy towards the target. The target acts as active element and answers with the signal back to the secondary radar. Which needs to be cooperative. As a result of integration of the target, the information of both the altitude and identification are obtained. The only problem with secondary radars is the expensive installation cost of electronic equipment [15].

2.5.2 Bistatic and Monostatic radar systems

Bistatic radar is a radar system that comprises of a transmitter and a receiver antennas that are separated by a distance that is equal to the distance of the expected target. In other hand a radar in which the transmitter and the receiver antennas are located at the same place is known as a monastic radar. Most long-range surface-to-air and air-to-air missiles employ the use of bistatic radar.

2.5.3 MIMO radar system

A Multiple-Input Multiple-Output (MIMO) radar is a system employing multiple transmitters and receivers, it is a subset of multistatic radar, is a system of multiple antennas in which each transmit antenna radiates an arbitrary waveform independently of the other transmitting antennas and each receiving antenna can receive these signals. Due to the different waveforms, the echo signals can be reassigned to the single transmitter [15].

2.5.4 Tracking radar

A tracking-radar system measures the coordinates of a target and provides data which may be used to determine the target path and to predict its future position. All or only part of the available radar data-range, elevation angle, azimuth angle, and Doppler frequency shift may be used in predicting future position; that is, a radar might track in range, in angle. In doppler, or with any combination. Almost any radar can be considered a tracking radar provided its output information is processed properly. But, in general, it is the method by which angle tracking is accomplished that distinguishes what is normally considered a tracking radar from any other radar[15].

2.5.5 Instrumentation radar

Instrumentation radars are radars that are designed to test rockets, missiles, aircraft, and ammunitions on government and private test ranges. They provide a variety of information including space, position, and time both in real-time and in the post-processing analysis.

2.5.6 Search radar

A search radar, also called surveillance radar, is the process of examining a volume of space with the objective of detecting targets in that volume. The search objectives usually include the search volume, and find their information, including range, angular position, and velocity. Depending on the radar design, different search patterns can be adopted, namely a two-dimensional fan beam, a stacked beam. In the case of a two-dimensional fan beam search radar, the beam width is wide enough to cover the desired search volume along that coordinate while steering in azimuth. In the case of the stacked-beam pattern, the beam is steered in azimuth and elevation [15].

2.5.7 Imaging radar / NO-Imaging radar

Imaging radar sensor measures two dimensions of co-ordinates at least for calculating of map by the radar bream. Imaging radar forms a picture of the observed object or area. Imaging radars have been used to map the earth, other planets asteroids, and other celestial objects and to categorize targets for military systems [16].
No-imaging sensors take measurements in one linear dimension, as opposed to the dimensional representation of imaging sensors, typically implementations of no-imaging radar system are speed gauges and radar altimeters, these are also called scatterometers since they measure the scattering properties of the object or region being observed non-imaging secondary radar application are immobilized in some recent private cars

2.5.8 Weather radar

Weather radar (also known as Doppler weather radar) is an instrument that sends pulses of electromagnetic energy into the atmosphere to find precipitation, determine its motion and intensity, and identify the precipitation type such as rain, snow or hail. When the electromagnetic pulse strikes an object such as a raindrop or a snowflake, the wave reflects back to the radar with data that can be analyzed by meteorologists. Meteorologists can use this information to determine specific areas where dangerous weather conditions exist. As a result, radar can be an exceptional tool in a meteorologist's arsenal for helping to protect life and property [17].

2.5.9 Pulse radar

Pulse radar sets transmit a high-frequency impulse signal of high power. After this impulse signal, a longer break follows in which the echoes can be received. Before a now transmitted signal is sent out. Direction, distance and sometimes if necessary the height or altitude of the target can be determined from the measured antenna position and propagation time of the pulse-signal these classically radar sets transmit a very short pulse (to get a good range resolution) with an extremely high pulse-power (to get a good maximum range).

2.5.10 Maritime navigation radar

The radar is one of the most important elements of marine electronics on any ship, it is designed to detect and track sea targets at a great distance, it goes without saying that it is of great practical value to mariners. Its main purpose is to help prevent a collision when navigating in darkness, fog, or other situations with limited visibility. Radar is also useful for monitoring the position and movement of ships when crossing narrow lanes or congested waterways, regardless of visibility. The radar also helps determine the position of ships in relation to landmasses or islands, even when you are out of sight with the naked eye. The two fundamental characteristics of a marine radar are the transmitter power and beam angle. The power can vary between 4 and 25 kilowatts, the power is an essential factor in determining the performance of a radar in bad weather. The higher the power of a radar, the better transmitter can see through dense fog and rain, and the farther the signal can reach. The beam angle is determined by the size of a radar antenna. A long antenna emits a narrow beam which can better distinguish objects close to each other that a shorter antenna. On the other hand, a short antenna produces a wider beam angle which allows the radar to scan a larger area than a long antenna at a time. The specific environment for maritime surveillance radars is sea clutter, the characterization of unwanted echoes reflected from the sea surface, is an important step in the performance analysis of different remote sensing systems, for many applications [18]:

- Detection, recognition and identification of objects present on the sea surface (periscope, low-flying plane or missile) to ensure coastal safety.
- Identification of small boats, buoys, icebergs or oil slicks.
- Surveillance and intervention on vessels operating in illegal fishing.
- The exploitation of signals reflected from the sea surface to obtain oceanographic characteristics of seawater.

2.5.11 Classification by Frequency Band

Although radars usually use a radio frequency between 220 and 35 000 MHz, of the electromagnetic spectrum, they can also function in any spectral region. A few types of radar are

found in lower band, except in cases where special propagation and target characteristics dictate their use. Early in the development of radar, a letter code was employed to designate the radar frequency band. At the upper frequency end of the spectrum, L-band, S-band, C-band, and X-band radars are used where the size of the antenna constitutes a physical limitation. The other higher frequency bands (Ku, K, and Ka) suffer severe weather and atmospheric attenuation. Further information on common usage and applications of the radar frequency bands, as defined by IEEE, are summarized in table 2.1 [11].

Band	Frequency (GHz)	Usage
HF	0.003–0.03	OTH surveillance
VHF	0.03–0.3	Very long-range surveillance
UHF	0.3–1	Very long-range surveillance
L	1–2	Long-range military and air traffic control search
S	2–4	Medium range surveillance, and meteorological
C	4–8	Search and fire control radars, weather detection
X	8–12.5	Short-range tracking, missile guidance, marine radar
K_u **(under K band)**	12.5–18	High-resolution mapping, satellite altimetry
K	18–26.5	Police speed-measuring, airport surface detection
K_a **(above K band)**	26–40	Very high-resolution mapping, airport surveillance
MM-Wave	40–300	Laser range finders and optical targeting systems. Experiments

Table 2.1: Radar frequency bands and usages.

2.5.12 Classification by waveforms and Pulse rate

The most popular type of radar is the pulsed radar. The waveform of a pulsed radar is usually represented by the pulse duration T, the pulse repetition interval (PRI) T, or the pulse repetition frequency (PRF). PRI is the time interval between two adjacent pulses. PRF is the rate that pulses repeat per second and is equal to the inverse of PRI. In general, radar of this type using a pulse train as shown in figure 2.3

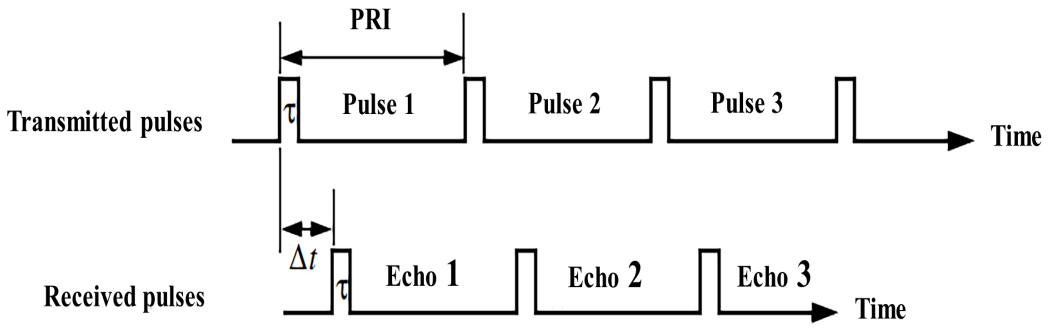

Figure 2.3: Train of transmitted and received pulses.

PRF is normally expressed as the number of pulses transmitted in 1 s and is therefore denoted in Hertz or pps (pulses per second). Typical values for a marine radar are 1000–3000 pps. The pulse repetition interval (PRI) is the time interval between pulses. It should be noted that PRF and PRI effectively refer to the same feature and are simply related by the expression PRF=1/PRI. The second type of classification is CW radars, where the radar continuously emits electromagnetic energy from an antenna and receives using a second antenna separate from the first, this type is used to track and guide missiles. Unmodulated CW radars can accurately measure target radial velocity and angular position, utilizing some form of time variant modulation, the range information can be extracted [11].

2.6 Different types of noise

In Radar system, there are many sources of unwanted signals, that radar need to be able to ignore them, in order to focus only on the targets of interest. These signals can be passive (Internal) as thermal noise and external such as interference or clutter. The power of clutter is much higher than that the thermal noise.

2.6.1 Thermal noise

Thermal noise is always present in the electrical radar equipment used and is one of the major sources of noise that can affect the weak levels of radar signals at their source.

2.6.2 Radar clutter

Radar clutter is defined as any unwanted radar echo that can clutter the radar output and make the detection of a wanted target difficult. The presence of clutter always degrades of radar performance as the clutter returns compete with target returns in the radar detection process. When clutter echoes are sufficiently intense, they can impose serious limitations in the performance of the radar operations. And in such circumstances, the optimum radar waveform and receiver design can be quite different than when receiver noise alone is the dominant effect. Clutter may be divided into sources distributed over a surface, within a volume, or concentrated at discrete points. Ground or sea returns are typical surface clutter. Returns from geographical land masses are generally stationary; however, the effect of wind on trees. In the air, the most significant problem is weather clutter, which can be produced from rain or snow and can have a significant Doppler content. Birds, windmills, and individual tall buildings are typical point clutter and are not extended in nature. Birds and insects produce clutter, which can be very difficult to remove because the characteristics are very much like aircraft. Clutter can be fluctuating or non-fluctuating. Ground clutter is generally non-fluctuating in nature because the physical features are normally static. On the other hand, weather clutter is mobile under the influence of wind and is generally considered fluctuating in nature. Clutter can be defined as homogeneous if the density of all the returns

is uniform. Most types of surface and volume clutter are analyzed on this basis, however, in practice this simplification does not hold true in all cases. Non-homogeneous clutter is non-uniform clutter where the amplitude of the clutter varies significantly from cell to cell [11]. The raison of distributive nature of the clutter, the measurement of backscatter echo from such clutter is generally given in terms of RCS density. For surface clutter, we define an RCS per unit area:

$$\sigma = \frac{\sigma_c}{A_c} \tag{2.12}$$

Where $\sigma_c$is the RCS from the area A_c. The advantage of using this expression to describe distributed surface clutter is that it is usually independent of area Ac. For volume distributed clutter a cross section per unit volume, or reflectivity is defined as:

$$\eta = \frac{\sigma_c}{V_c} \tag{2.13}$$

where σ_c in this case is the radar cross section from the volume V_c.

2.6.3 Volume Clutter

Weather or chaff is typical volume clutter. In the air, the most significant problem is weather clutter. This can be produced from rain or snow and can have a significant Doppler content.

2.6.4 Surface clutter

Ground or sea returns are typical surface clutter. Returns from geographical land masses are generally stationary, however, the effect of wind on trees etc. This Doppler shift is an important method of removing unwanted signals in the signal processing part of radar system. Clutter returned from the sea generally also has movement associated with the waves.

2.6.5 Sea clutter

Sea clutter suffers temporal and spatial variations, and is largely dependent on wave height. Several quantities have been used to describe wave height including sea state, average wave height, peak wave height, wind speed, frequency, polarization, radar look direction relative to wave direction, and grazing angle. A number of features are used to describe the sea clutter including [15]:

- The area reflectivity σ.
- The amplitude distribution of the clutter or power..
- The spectrum of the clutter returns..
- The spatial variation of the clutter return..

- The polarisation scattering matrix.
- The discrete clutter spikes.

The amplitude statistics of sea clutter are described using families of PDFs, and their derived functions. The manner in which these amplitude fluctuations vary with time is characterized by the spectrum of the returns.

2.6.6 Sea surface

Observations of radar sea clutter are usually associated with particular characteristics of the sea surface and the environment, such as sea waves, sea swell or wind speed. Some of the basic terms used to describe the sea surface are presented here [15]:

- Wind wave: a wave resulting from the action of the wind on a water surface.
- Gravity wave: a wave whose velocity of propagation is controlled primarily by gravity, water waves of a length greater than 5 cm are considered gravity waves.
- Capillary wave also called ripple or capillary ripple: a wave whose speed of propagation is controlled primarily by the surface tension of the liquid in which the wave is traveling, water waves of a length of less than 2.5 cm are considered capillary waves.
- Fetch also called generating area: an area of ocean, sea, or lake surface over which the wind blows in an essentially constant direction, thus generating waves.
- Duration: the length of time the wind blows in essentially the same direction over the fetch.
- Fully developed sea also called a fully arisen sea: the maximum height at which ocean waves can be generated by a given wind force blowing a sufficient amount, regardless of the duration.
- Sea state: a description of the properties of sea surface waves at a given time and place, it is related to the Beaufort scale which describes the state of the sea.

2.6.7 Sea clutter reflectivity

Radar backscatter from the sea is derived from a complex interaction between incident electromagnetic waves and the sea surface. There are many theoretical models for backscatter based on different descriptions of the rough surface and approximations to the scattering mechanism. The essential feature of radar sea clutter, and important for radar performance evaluations, is its apparent reflectivity. Sea clutter reflectivity depends on many factors, including sea state, wind velocity, grazing angle, polarization, radar frequency and many other factors. Empirical models often present reflectivity as a function of the sea state. However, this is not always a reliable indicator as it is dominated by the wave height of long

waves and sea swell. Local winds cause surface roughness of small scale, which quickly responds to changes in wind speed and back scattering change. A strong swell without a local wind gives low reflectivity, while a strong local wind gives a strong backscatter from a relatively flat sea. Further deviation from a simple sea state trend may be caused by propagation effects such as ducting, which can affect the illumination grazing angle [15].

2.7 Detection process

The main and the primary action of radar system is to detect whether the target is present or not. In practice the receiver signal is corrupted by thermal noise and interferences. In search mode, the radar system is programmed to change the position of the antenna beam in a specific sequence to scan every possible position in space in search of a target. The detection is a process by which the echo signal of each potential target location is compared to an estimated threshold level from its surroundings to determine whether the signal is sufficiently high to be considered as a target of interest. The echo signal exists alongside interfering signals called "clutter" which comes in many forms, such as electromagnetic waves reflected from uninteresting objects (land, atmosphere, sea, clouds, rain, birds, insects...). Clutter can also comes in the form of unintentional external electromagnetic waves from other artificial sources, or waves emitted by special systems to mask the targets that the radar can detect, and internal and external thermal noise. Considering the fact that the clutter is statistically non-stationary and has unknown powers due to the random fluctuation of electrical energy, crossing the detection threshold can be subject to errors and false alarms, which greatly affects the detection performance, especially in conventional radars that use fixed detection thresholds. We define the Probability of False Alarm (Pfa) the probability of crossing the threshold by clutter or thermal noise alone. The Probability of Detection (Pd) is defined as the probability of crossing the threshold by the signal from the potential target alone or with clutter. To reduce Pfa caused by unwanted strong signals and improve Pd performance, modern radars use adaptive threshold strategies to maintain a CFAR, this process is performed just before the detection decision is made. In adverse weather conditions, clutter becomes the dominant source and its amplitude may be greater than the target signal, in this case, spectral signal processing such as Moving Target Indication (MTI) is often used to reduce the noise level below that of the target signal. In cases where the dominant interference is jamming and its level exceeds that of the target, the angle of arrival processing can often be used. The systems that undergo a significant clutter and jamming interference may use a combination of both MTI and angle of arrival processing, called Space Time Adaptive Processing (STAP) [12, 15]. In addition, optimal detection strategies, such as Bayes or Neyman Pearson (NP), must be developed based on an accurate modeling of echo signals, capable of operating at all times and in all conditions regardless of the environment in which the radar is operating.

Chapter 3

Iterative maximum likelihood estimation of the compound inverse Gaussian clutter parameters

Contents

Abstract

In this chapter, we analyze a cost-effective method for estimating the parameters of the compound inverse Gaussian distributed clutter. Under the assumption of the absence of thermal noise, an iterative maximum likelihood estimator (IMLE) is proposed and compared with existing MLE, the [zlog(z)] estimator, the non-integer order moments estimator and the higher order moment estimator. The results obtained show that the IMLE method outperforms all the other methods and has similar estimation performance than the MLE method but requires lower computational time.

3.1 Introduction

Compound Gaussian (CG) models with different textures have been widely used for the modeling of high resolution sea clutter. Among these compound models, the compound inverse Gaussian (CIG) clutter characterized by an inverse Gaussian texture has been validated experimentally using real data [19]. The parameter estimation of these statistical distributions from measured samples is an important task in order to set detection thresholds and regulate the false alarm rate. Several methods have been proposed to estimate the parameters of CIG. These methods are [zlog(z)], NIOM, MoM and Maximum Likelihood estimation (MLE) [6, 7, 8]. MLE is the most straightforward and generally the most accurate method for parameter estimation. However, this method involves computationally intensive numerical methods to solve non-linear equations. For this, more tractable methods were proposed in the literature. In [6], *Iskander* and *Zoubir* proposed a method based on higher-order and fractional sample moments. This method is computationally inexpensive and under some conditions leads to accurate estimates. *Belleri* et *al* in [7] developed the MLE and the method of fractional moments to estimate the parameters of a distribution with an inverse Gamma texture. *Blacknell* and *Tough* analysed the performance of the [zlog(z)] estimator for the K distributed clutter [8]. In [20], *Shui* et *al*. proposed an iterative MLE for parameter estimation of the CIG model in the case without outliers and an outlier-robust bipercentile estimator in the case of the presence of outliers. *Mezache* et *al* analysed and compared different estimators for the CIG distribution taking into account the presence of thermal noise [9, 21]. In this chapter, we propose the IMLE method to estimate the scale and shape parameters of CIG in the absence of thermal noise and we compare with other estimators disccussed in [9]. The results showed that the IMLE has the best performance compared to [zlog(z)],MoM, INOM and MLE method, but the IMLE has similar estimation performance than the MLE method but requires lower computational time. This chapter is organized as follows: section 3.2 presents the Gaussian distributions. Section 3.3 describes the Non-Gaussian distributions and section 3.4 includes Compound Gaussian distributions. In section 3.5, we present parameters estimation methods . Section 3.6 proposes an Iterative MLE (IMLE) method for the CIG distribution. Section 3.7 discusses the results obtained using the proposed IMLE method compared te the exsiting methods and lastely section 3.8 presents our conclusions.

3.2 The Gaussian distributions

This kind of distributions are used to describe low-resolution sea clutter and it is always modeled by Exponential or Rayleigh distribution, which have one parameter (mono-parameteric).

3.2.1 The Exponentiel distribution

A random variable X has an exponential distribution with parameter β, $\beta > 0$, if its probality density function (pdf) is given by [14]

$$\begin{cases} f_X(x) = \dfrac{1}{\beta} e^{-\frac{1}{\beta}(x-a)}; x \geq a, -\infty < a < \infty \\ o; otherwise \end{cases} \tag{3.1}$$

If we set $a = 0$ and $\alpha = \frac{1}{\beta}$, then $f_X(x)$, becomes

$$\begin{cases} f_X(x) = \alpha e^{-\alpha x}; x \geq 0 \\ 0; otherwise \end{cases} \tag{3.2}$$

The mean and variance of X are:

$$E[X] = \beta = \frac{1}{\alpha} \tag{3.3}$$

$$\text{var}[X] = \beta^2 = \frac{1}{\alpha^2} \tag{3.4}$$

3.2.2 The Rayleigh distribution

The Rayleigh distribution, which is frequently used to model the statistics of signals, finds its application in many radar and communication problems. It's pdf is given by [14]

$$\begin{cases} f_Y(y) = \dfrac{y}{\sigma^2} \exp\left(-\dfrac{y}{2\sigma^2}\right); y \geq 0 \\ 0; otherwise \end{cases} \tag{3.5}$$

It can be shown that the moments of order k of the Rayleigh distribution are given by

$$E\left[Y^k\right] = \left(2\sigma^2\right)^{\frac{k}{2}} \Gamma\left(1 + \frac{k}{2}\right) \tag{3.6}$$

3.3 The Non-Gaussian distributions

In a high resolution radar system, however, a given range cell may contain only a few independent scattering structures. In this case, the arguments put forward in support of

the Gaussian model may break down as the radar effectively resolves some of the larger scale structure of the sea surface. The clutter observed in this case is subject to much greater fluctuations (sea spikes) than are seen in Gaussian clutter. Thus, the improvement in signal–to-noise ratio and potential detection achieved by increasing the resolution of the system can be more than offset by the clutter becoming effectively target-like and regularly exceeding thresholds based on a Gaussian model of the clutter. Realistic non-Gaussian clutter models are needed if the performance lost to the sea spikes is to be understood and redeemed. This kind of distributions have generally two parameters, which are the shape and the scale parameter. The Non-Gaussian distributions are described by two types that are the Non-Gaussian distributions and Compound Gaussian distributions.

3.3.1 The Log-normal distribution

A random variable X has a log-normal distribution if its pdf is given by [14]

$$\begin{cases} f_Y(y) = \dfrac{1}{\sqrt{2\pi}\sigma} \exp\left(-\dfrac{\ln^2\left(\frac{x}{x_m}\right)}{2\sigma^2} \right); x \geq 0 \\ 0; otherwise \end{cases} \tag{3.7}$$

Where x_m is the median of X and σ^2 is the variance of the generating normal distribution.

3.3.2 The Weibull distribution

A random variable X has a Weibull distribution, if its probability density function is given [22]

$$\begin{cases} f_X(x) = abx^{(b-1)} e^{-ax^b}; x > 0, a > 0, b > 0 \\ 0; otherwise \end{cases} \tag{3.8}$$

Where a is referred to as the scale parameter and b is the shape parameter. Note that for $b = 1$, we obtain $f_X(x) = ae^{-ax}$, $x > 0$, and $a > 0$, which is the exponential distribution given in (3.2).When $b = 2$, the Weibull density function becomes Rayleigh density function defined in (3 .5) with $a = 1/2\sigma^2$.

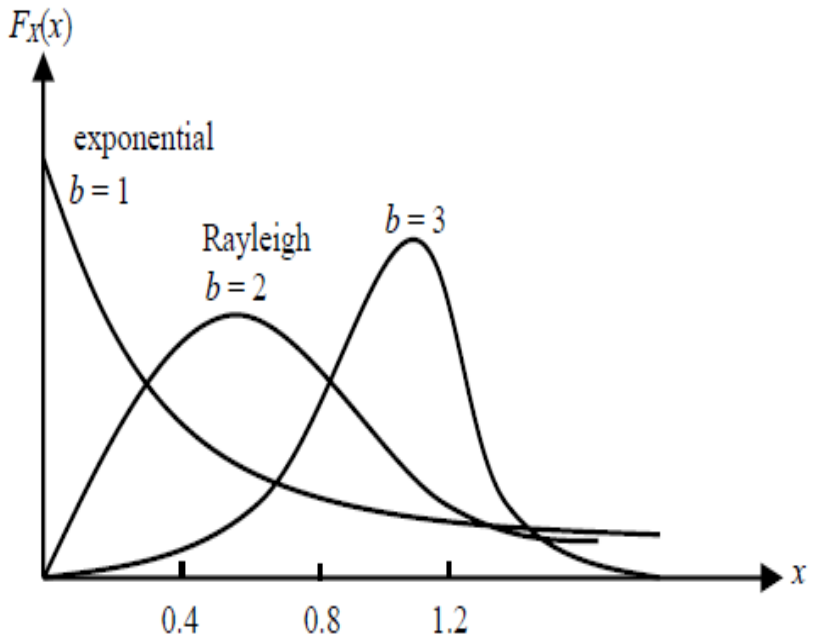

Figure 3.1: The Weibull distribution

The mean and variance of X are given by

$$E[X] = a^{-\frac{1}{b}}\Gamma\left(1+\frac{1}{b}\right) \tag{3.9}$$

And,

$$\text{var}(x) = a^{-\frac{2}{b}}\left\{\Gamma\left(1+\frac{2}{b}\right) - \left[\Gamma\left(1+\frac{1}{b}\right)\right]^2\right\} \tag{3.10}$$

3.3.3 The Pareto distribution

A random variable X has a Pareto distribution, if its pdf is given by [14]

$$\begin{cases} f_X(x) = \dfrac{\alpha\beta^{\alpha}}{x^{\alpha+1}}; x > 0, \alpha > 0 and \beta > 0 \\ 0; otherwise \end{cases} \tag{3.11}$$

Where α is the shape parameter and β represents the scale parameter.

3.4 Compound Gaussian distributions

Compound Gaussian (CG) model which was originally proposed for use in sea-clutter by Ward [5]. This model includes a temporal or fast varying component known as speckle which relates to the Bragg scattering (Bragg scattering occurs when the radar wavelength is resonant with the sea wave),and a slowly varying component which captures the underlying

swell and models the texture. The CG model is a multi-parameter PDF which is built up using the Generalized Gamma (GG) distribution. Both the speckle and texture component of the compound clutter are described using the GG pdf. Some of them are:

3.4.1 The K-distribution

The K-distribution has arisen mainly to represent radar sea clutter. A random variable X with probability density function [14]

$$\begin{cases} f_X(x) = \dfrac{4}{b\Gamma(\nu)}\left(\dfrac{x}{b}\right)^{\nu} K_{\nu-1}\left(\dfrac{2}{b}x\right); x > 0 \\ o; otherwise \end{cases} \tag{3.12}$$

$K_\nu(x)$ Is the modified Bessel function, b is the scale parameter and ν is the shape parameter. It is known from radar detection that the K-distribution results from a function of two random variables given by

$$X = ST \tag{3.13}$$

Where S, known as speckle, obeys to a Rayleigh distribution given by

$$f_{(s)}(s) = 2se^{-s^2} \tag{3.14}$$

and T, known as texture, is Gamma distributed and given by

$$f_T(t) = \frac{2}{b^\nu \Gamma(\nu)} t^{2\nu-1} e^{-\frac{t^2}{b^2}} \tag{3.15}$$

The total pdf $f_X(x)$ is defined in terms of conditional probabilities as:

$$f_X(x) = \int_0^\infty f_{X\backslash T}(x\backslash t) f_T(t) dt \tag{3.16}$$

Where,

$$f_{X\backslash T}(x\backslash t) = \frac{2x}{t^2} e^{-\frac{x^2}{t^2}} \tag{3.17}$$

Substituting (3.17) and (3.15) into (3.16) and solving the integral, the authors in reference [5] obtained:

$$E\left[X^k\right] = b^k \frac{\Gamma\left(\nu + \frac{k}{2}\right)\Gamma\left(1 + \frac{k}{2}\right)}{\Gamma(\nu)} \tag{3.18}$$

Where, $E\left[X^k\right]$ is the moment of order k.

3.4.2 Compound Inverse Gaussian Distribution(CIG)

A random variable X obeying to a CIG model is characterized by a mixture of two components having the following representation:

$$X = \sqrt{y}c \tag{3.19}$$

Where c is a zero-mean complex random variable, referred to as a speckle and y is a positive random variable referred to as texture [19]. If Y is a random variable representing the texture component, the overall probability density function (pdf) of X is given by

$$P_X(x) = \int_0^\infty P(x\backslash y)P(y)dy \tag{3.20}$$

Where,

$$\begin{cases} P(x\backslash y) = \dfrac{\pi x}{2y^2}\exp\left(-\dfrac{\pi x^2}{4y^2}\right) \\ P(y) = \dfrac{\lambda^{\frac{1}{2}}}{\sqrt{2\pi}y^{\frac{3}{2}}}\exp\left(-\lambda\dfrac{(y-\mu)^2}{2\mu^2 y}\right), 0 < y < \infty \end{cases} \tag{3.21}$$

λ is the shape parameter and μ is the mean. The first and second-order of moments were found the CIG clutter in [9]:

$$m_1 = \mu \tag{3.22}$$

$$m_2 = \frac{(\lambda+\mu)\mu^2}{\lambda} \tag{3.23}$$

3.5 Parameters Estimation methods

The detection process is related to the parameters of the clutter model used in the radar system. We assume that the receiver has made a decision in favor of the true hypothesis, but some parameter associated with the signal may not be known. The goal is to estimate those parameters in an optimum fashion based on a finite number of samples of the signal.
Let $Y_1, Y_2, ..., Y_K$ be K independent and identically distributed (IID) samples of a random variable Y, with some density function depending on an unknown parameter θ.Let $y_1, y_2, ..., y_k$ be the corresponding values of samples $Y_1, Y_2, ..., Y_K$ and $g(Y_1, Y_2, ..., Y_K)$, a function (a statistic) of the samples used to estimate the parameter θ [14].

$$\widehat{\theta} = g(Y_1, Y_2, ..., Y_K) \tag{3.24}$$

Several methods were proposed to estimate the parameter for distributions some of them are:

3.5.1 Maximum Likelihood Estimation (MLE)

The procedure commonly used to estimate nonrandom parameters is the maximum likelihood (ML) estimation. Let $Y_1, Y_2, ..., Y_K$ be K observations of the random variable Y, with sample values $y_1, y_2, ..., y_k$. These random variables are IID. Let $f_{Y\backslash\Theta}(y\backslash\theta)$ denotes the conditional density function of the random variable Y. Note that the density function of Y depends on the parameter θ, which needs to be estimated. The likelihood function, $L(\theta)$, is

$$L(\theta) = f_{Y_1, Y_2, ...Y_{K\backslash\Theta}}(y_1, y_2, ...y_k\backslash\theta) = f_{Y\backslash\Theta}(y\backslash\theta) \tag{3.25}$$

$$= \prod_{k=1}^{K} f_{Y_K\backslash\Theta}(y_k\backslash\theta) \tag{3.26}$$

The value $\hat{\theta}$ that maximizes the likelihood function is called the maximum likelihood estimator of θ. In order to maximize the likelihood function, standard techniques of calculus may be used. Because the logarithmic function lnx is a monotonically increasing function of x, maximizing $L(\theta)$ is equivalent to maximizing $\ln L(\theta)$. Hence, it can be shown that a necessary but not sufficient condition to obtain the ML estimates $\hat{\theta}$ is to solve the likelihood equation [14].

$$\frac{\partial}{\partial\theta} \ln f_{Y\backslash\Theta}(y\backslash\theta) = 0 \tag{3.27}$$

3.5.2 Method of Moments (MoM) or Higher order Moment (HOME)

Let $M_1, M_2, ..., M_n$ be independent random variables having a common distribution possessing a mean μ_M . Then the sample means converge to the distributional mean as the number of observations increase [9].

$$\hat{M}_n = \frac{1}{n} \sum_{i=1}^{n} M_i, n \Rightarrow \infty \tag{3.28}$$

To show how MoM determines an estimator, we first consider the case of one parameter. We start with independent random variables $X_1, X_2, ..., X_n$ chosen according to the probability density $f_X(x\backslash\theta)$ associated to an unknown parameter value θ. The common mean of the X_i, is a function $K(\theta)$ of θ, then

$$\mu_M = \int_{-\infty}^{\infty} x f_X(x\backslash\theta) dx = K(\theta) \tag{3.29}$$

The law of large numbers states that

$$\hat{X}_n = \frac{1}{n}\sum_{i=1}^{n} X_i = \mu_M, n \Rightarrow \infty \tag{3.30}$$

3.5.3 Method of Non-Integer Moments (NIOM)

This method is based on the calculation of the moment's expression of non-integer order r denoted by $\langle X^r \rangle$ [9].

$$\langle X^r \rangle = \int_0^\infty X^r f_X(x) dx \tag{3.31}$$

3.5.4 Method of [zlog(z)]

The [zlog(z)] method requires the combination of the means of the random variables z, $log(z)$ and $zlog(z)$ denoted by $\langle z \rangle$, $\langle logz \rangle$ and $\langle zlogz \rangle$ respectively[6]. Hence the $log(z)$ is calculated by [9]:

$$\langle \log(z) \rangle = \int_0^\infty f(y) \left[\int_0^\infty \log(z) f(z \backslash y, N) dz \right] dy \tag{3.32}$$

3.5.5 The Iterative MLE method (IMLE)

In some cases it is impossible to find exact values of the estimated parameters, for example, when the clutter is modeled by compound Gaussian as CIG. Otherwise, in general, one is interested in finding approximate solutions using some numerical methods. Like Iterative Maximum likelihood estimator (IMLE), this method is based on two different methods which are the MLE and MoM, where the algorithm of IMLE starts by MoM which is used as a first step that finds the estimation of the parameters and we use them as initial points. After that the second step is to estimate the parameters of the clutter using the algorithm of MLE, finally the IMLE is derived from the two previous steps for K iterations where,

$$\hat{x}(k) = \hat{x}(k-1) \tag{3.33}$$

Our first contribution is based on this estimator. We used it to improve the MLE etsimator in terms of computational time. The next section presents the IMLE method for CIG distribution.

3.6 Proposed Iterative MLE (IMLE) method for the CIG distribution

Given M independent and identically distributed $X_m = 1,2,...M$, the statistical first and second-order sample moments are given by:

$$\hat{m}_1 = \frac{1}{M}\sum_{i=1}^{M} X_m \tag{3.34}$$

$$\hat{m}_2 = \frac{1}{M}\sum_{i=1}^{M} X^2{}_m \tag{3.35}$$

From (3.34) and (3.35), the mean and the shape parameters are estimated using the method of moment (MoM) as:

$$\hat{\mu}_{MOM} = \hat{m}_1 \tag{3.36}$$

$$\hat{\lambda}_{MOM} = \frac{2\hat{m}_1^3}{\hat{m}_2 - 2\hat{m}_1^2} \tag{3.37}$$

In [9], the authors used the MLE to estimate the two parameters of CIG , they found two equations which are:

$$\frac{M}{\hat{\mu}} - \sum_{i=1}^{M}\left(\frac{1}{\hat{\lambda}+2X_i} + \frac{\hat{\lambda}+X_i}{\hat{\mu}\sqrt{\hat{\lambda}^2+2\hat{\lambda}X_i}} - \frac{\hat{\mu}X_i + \sqrt{\hat{\lambda}}\left(\hat{\lambda}+2X_i\right)^{\frac{3}{2}}}{\sqrt{\hat{\lambda}}\left(\hat{\lambda}+2X_i\right)\left(\hat{\mu}\sqrt{\hat{\lambda}}+\hat{\lambda}\sqrt{\hat{\lambda}+2X_i}\right)}\right) = 0 \tag{3.38}$$

$$M - \sum_{i=1}^{M}\frac{\hat{\lambda}+2X_i}{\hat{\mu}+\sqrt{\hat{\lambda}^2+2\hat{\lambda}X_i}} = 0 \tag{3.39}$$

From equation (3.38) we obtained:

$$\frac{M}{\hat{\mu}} = \sum_{i=1}^{M}\left(\frac{1}{\hat{\lambda}+2X_i} + \frac{\hat{\lambda}+X_i}{\hat{\mu}\sqrt{\hat{\lambda}^2+2\hat{\lambda}X_i}} - \frac{\hat{\mu}X_i + \sqrt{\hat{\lambda}}\left(\hat{\lambda}+2X_i\right)^{\frac{3}{2}}}{\sqrt{\hat{\lambda}}\left(\hat{\lambda}+2X_i\right)\left(\hat{\mu}\sqrt{\hat{\lambda}}+\hat{\lambda}\sqrt{\hat{\lambda}+2X_i}\right)}\right) \tag{3.40}$$

$$\frac{M}{\hat{\mu}} - \sum_{i=1}^{M}\left(\frac{1}{\hat{\lambda}+2X_i}\right) + \sum_{i=1}^{M}\left(\frac{\hat{\mu}X_i + \sqrt{\hat{\lambda}}\left(\hat{\lambda}+2X_i\right)^{\frac{3}{2}}}{\sqrt{\hat{\lambda}}\left(\hat{\lambda}+2X_i\right)\left(\hat{\mu}\sqrt{\hat{\lambda}}+\hat{\lambda}\sqrt{\hat{\lambda}+2X_i}\right)}\right) = \sum_{i=1}^{M}\left(\frac{\hat{\lambda}+X_i}{\hat{\mu}\sqrt{\hat{\lambda}^2+2\hat{\lambda}X_i}}\right) \tag{3.41}$$

$$\frac{M}{\hat{\mu}} - \sum_{i=1}^{M}\left(\frac{1}{\hat{\lambda}+2X_i}\right) + \sum_{i=1}^{M}\left(\frac{\hat{\mu}X_i + \sqrt{\hat{\lambda}}\left(\hat{\lambda}+2X_i\right)^{\frac{3}{2}}}{\sqrt{\hat{\lambda}}\left(\hat{\lambda}+2X_i\right)\left(\hat{\mu}\sqrt{\hat{\lambda}}+\hat{\lambda}\sqrt{\hat{\lambda}+2X_i}\right)}\right) = \sum_{i=1}^{M}\hat{\lambda}\left(\frac{\left(1+X_i/\hat{\lambda}\right)}{\hat{\mu}\sqrt{\hat{\lambda}^2+2\hat{\lambda}X_i}}\right) \quad (3.42)$$

Finally we obtained:

$$\hat{\lambda} = \frac{\frac{M}{\hat{\mu}} - \sum_{i=1}^{M}\left(\frac{1}{\hat{\lambda}+2X_i}\right) + \sum_{i=1}^{M}\left(\frac{\hat{\mu}X_i+\sqrt{\hat{\lambda}}\left(\hat{\lambda}+2X_i\right)^{\frac{3}{2}}}{\sqrt{\hat{\lambda}}\left(\hat{\lambda}+2X_i\right)\left(\hat{\mu}\sqrt{\hat{\lambda}}+\hat{\lambda}\sqrt{\hat{\lambda}+2X_i}\right)}\right)}{\left(\frac{\left(1+X_i/\hat{\lambda}\right)}{\hat{\mu}\sqrt{\hat{\lambda}^2+2\hat{\lambda}X_i}}\right)} \quad (3.43)$$

From (3.39) we obtained:

$$M = \sum_{i=1}^{M}\frac{\hat{\lambda}+2X_i}{\hat{\mu}\left(1+\left(\sqrt{\hat{\lambda}^2+2\hat{\lambda}X_i}/\hat{\mu}\right)\right)} \quad (3.44)$$

$$\hat{\mu} = \frac{\sum_{i=1}^{M}\left(\frac{\hat{\lambda}+2X_i}{1+\left(\sqrt{\hat{\lambda}^2+2\hat{\lambda}X_i}/\hat{\mu}\right)}\right)}{M} \quad (3.45)$$

We used the Moment-based estimates in (3.36) and (3.37) as initial points , an Iterative Maximum Likelihood is derived:

$$\hat{\mu}_{MOM} = \hat{\mu}_0 \quad (3.46)$$

$$\hat{\lambda}_{MOM} = \hat{\lambda}_0 \quad (3.47)$$

For K iterations, we obtained

$$\hat{\lambda}_k = \frac{\frac{M}{\hat{\mu}_0} - \sum_{i=1}^{M}\left(\frac{1}{\hat{\lambda}_{k-1}+2X_i}\right) + \sum_{i=1}^{M}\left(\frac{\hat{\mu}_0X_i+\sqrt{\hat{\lambda}_{k-1}}\left(\hat{\lambda}_{k-1}+2X_i\right)^{\frac{3}{2}}}{\sqrt{\hat{\lambda}_{k-1}}\left(\hat{\lambda}_{k-1}+2X_i\right)\left(\hat{\mu}_0\sqrt{\hat{\lambda}_{k-1}}+\hat{\lambda}_{k-1}\sqrt{\hat{\lambda}_{k-1}+2X_i}\right)}\right)}{\left(\frac{\left(1+X_i/\hat{\lambda}_{k-1}\right)}{\hat{\mu}_0\sqrt{\hat{\lambda}_{k-1}^2+2\hat{\lambda}_{k-1}X_i}}\right)} \quad (3.48)$$

$$\hat{\mu}_k = \frac{\sum_{i=1}^{M}\left(\frac{\hat{\lambda}_k+2X_i}{1+\left(\sqrt{\hat{\lambda}_k^2+2\hat{\lambda}_kX_i}/\hat{\mu}_{k-1}\right)}\right)}{M} \quad (3.49)$$

3.7 Results and discussions

To assess the effectiveness of the proposed method, simulation experiments are carried out and compared with the MLE, [zlog(z)], non-integer order moment estimator (NIOM) and higher order moment (HOME) or (MoM) in terms of the MSE and the computational time. The number of samples is $M = 1000$, $\mu = 1$ and λ varies from 0.1 to 1.5 with a step equal to 0.2. From Fig 3.2 , it is clear that the IMLE method has comparable performance compared to the MLE and outperforms all the other methods (lowest MSE). This gain in performance is more pronounced for spiky clutter; that is for values of λ close to 0.
On the other hand, from Table 3.1 which summarizes the computation time for the method considered above and for different values of λ , we observe that the IMLE method requires lower computation time than the MLE method. It is also worth noticing that the [zlog(z)], NIOM and HOME methods are less time consuming than the IMLE method but with less accuracy.
Where the computation time is calculated using machine of calculation that has the following characteristics:

- **Processor**: Intel(R) Core(TM) i5-3317U CPU @ 1.70GHZ 1.70GHZ.
- **RAM**: 6.00 Go.
- **System type**: Exploitation system 64 bits, processor x64.

Finally, Figure 3.3 compares the MSE of the IMLE and the HOME estimation methods for the parameter μ and different values of λ. The other methods use the same procedure for estimating as the HOME method. Here again, the IMLE method improves the accuracy of estimation compared to the HOME method.

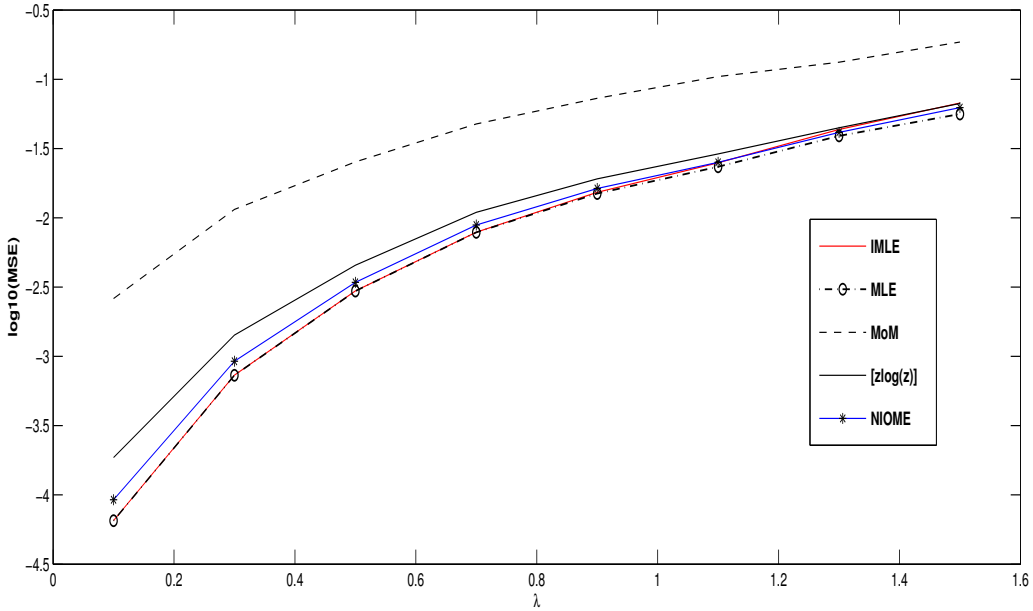

Figure 3.2: MSE estimates of the shape parameter λ of the CIG clutter.

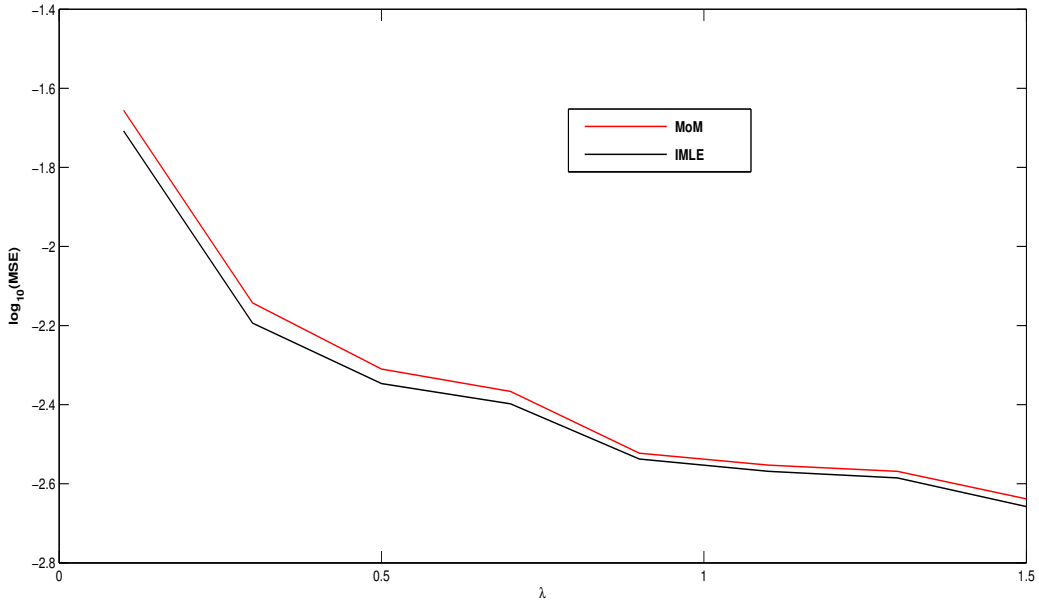

Figure 3.3: MSE estimates of the mean parameter μ of the CIG clutter.

Table 3.1: Computing time in seconds to estimate the shape parameter of IG-CG using different estimators

λ	$T_{MLE}(s)$	$T_{IMLE}(s)$	$T_{NIOME}(s)$	$T_{z[lig(z)]}(s)$	$T_{HOME}(s)$
0.1	0.0209	0.011	$5.7812\times10^{(-04)}$	0.0016	$1.5625\times10^{(-05)}$
0.3	0.0254	0.0039	$4.2188\times10^{(-04)}$	0.0014	$7.8125\times10^{(-05)}$
0.5	0.0271	0.0077	$4.8438\times10^{(-04)}$	0.0012	$7.8125\times10^{(-05)}$
0.7	0.0284	0.0118	$4.7187\times10^{(-04)}$	0.0013	$4.6875\times10^{(-04)}$
0.9	0.0300	0.0165	$4.6875\times10^{(-04)}$	0.011	$1.0938\times10^{(-04)}$
1.1	0.0296	0.0205	$4.375\times10^{(-04)}$	0.011	$6.25\times10^{(-05)}$
1.3	0.0307	0.0227	$7.0312\times10^{(-04)}$	0.011	$6.25\times10^{(-05)}$
1.5	0.0332	0.0232	$5.1563\times10^{(-04)}$	0.0014	$1.25\times10^{(-04)}$

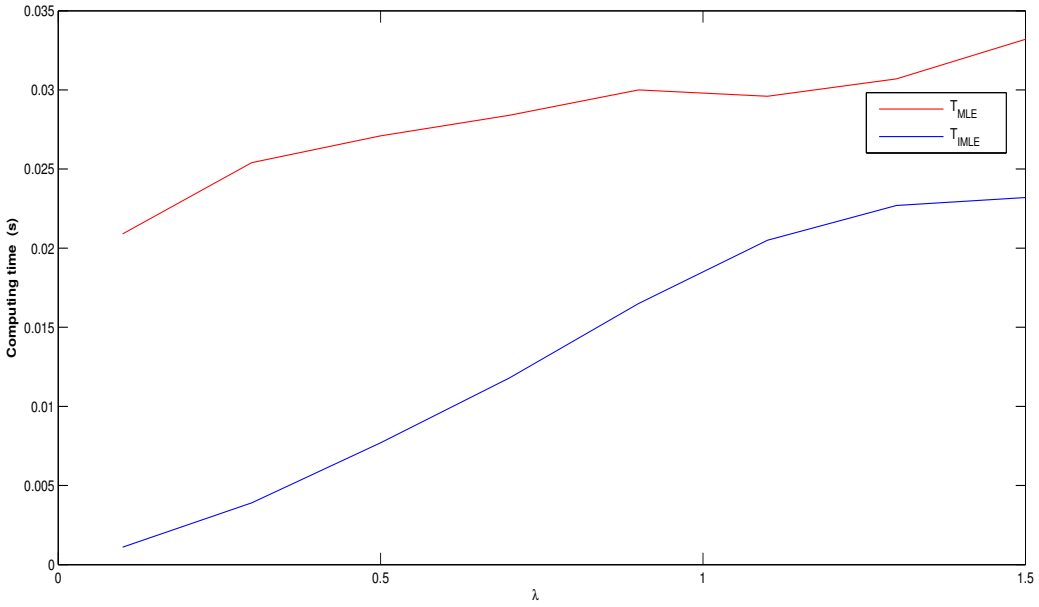

Figure 3.4: Computing time in seconds to estimate the shape parameter of IG-CG using MLE and IMLE methods.

Figure 3.4 presents the computation time in seconds to estimate the shape parameter of IG-CG using MLE and IMLE methods.it shows that the MLE method requires higher computation time than the IMLE method.

The simulation is carried out for different values of μ and λ, we obtained:

For $\mu = 0.3$, λ varies from 0.1 to 1.5 with a step equal to 0.2 and the number of samples $M = 1000$.

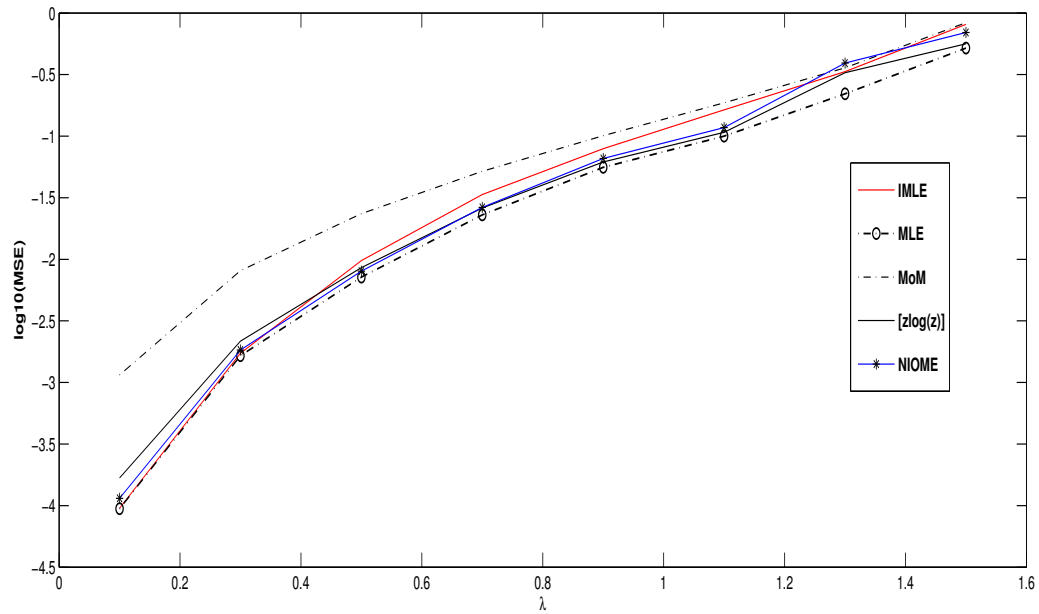

Figure 3.5: MSE estimates of the shape parameter λ of the CIG clutter.

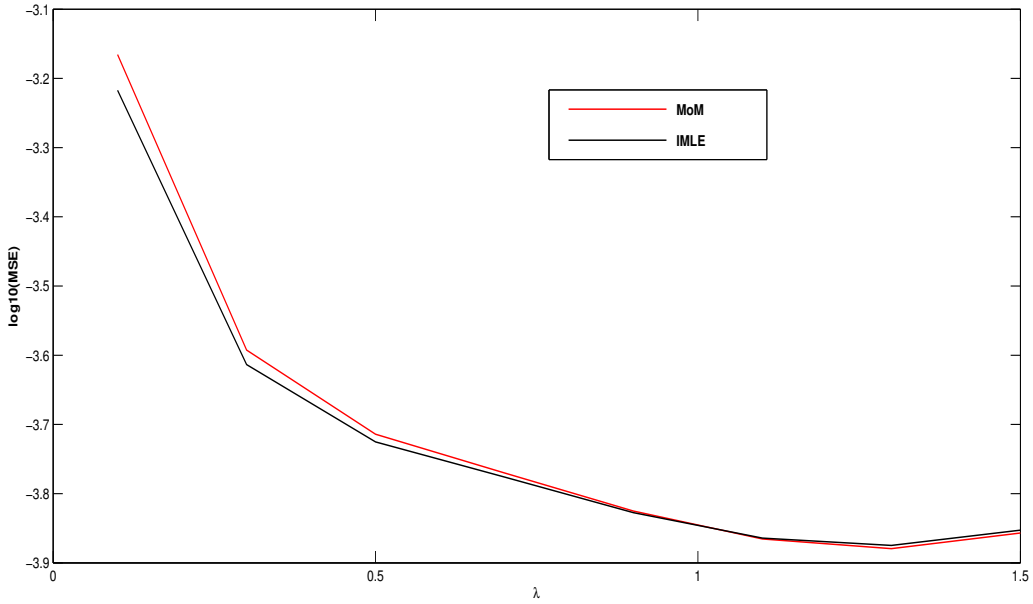

Figure 3.6: MSE estimates of the mean parameter μ of the CIG clutter.

For $\mu = 0.5$, λ varies from 0.1 to 1.5 with a step equal to 0.2 and the number of samples $M = 1000$.

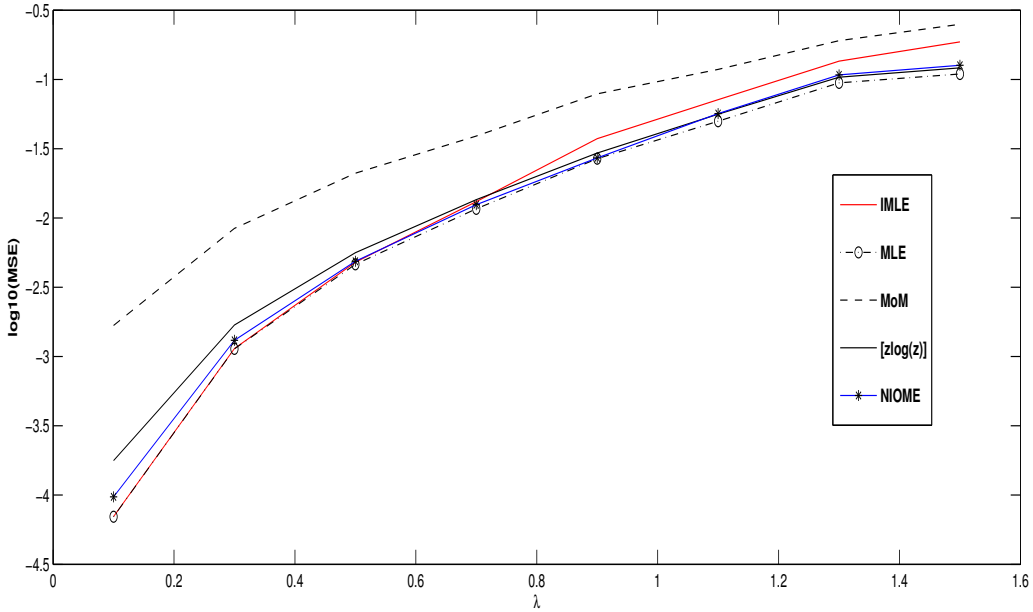

Figure 3.7: MSE estimates of the shape parameter λ of the CIG clutter.

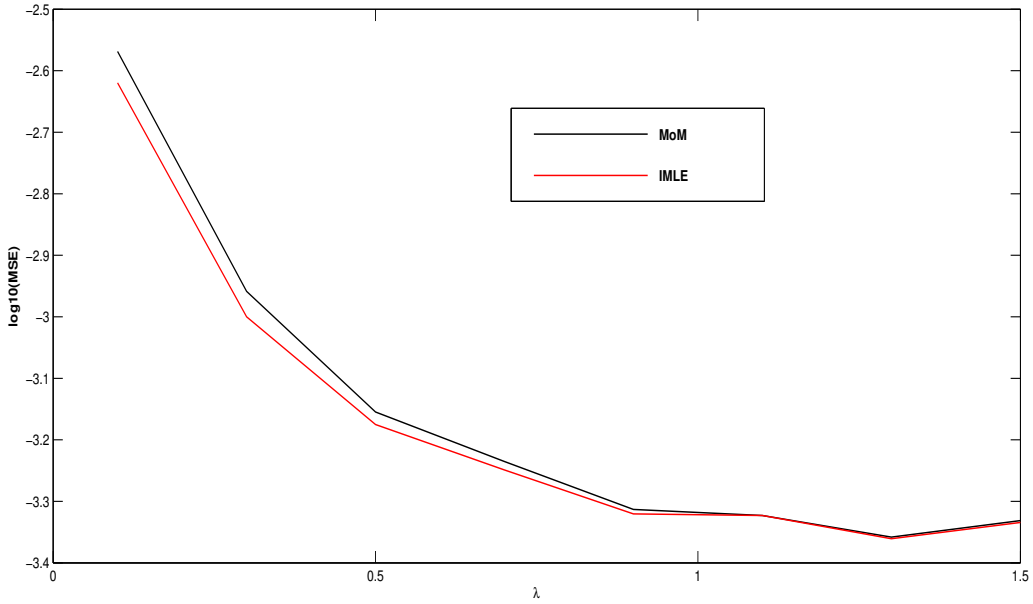

Figure 3.8: MSE estimates of the mean parameter μ of the CIG clutter.

For $\mu = 0.7$, λ varies from 0.1 to 1.5 with a step equal to 0.2 and the number of samples $M = 1000$.

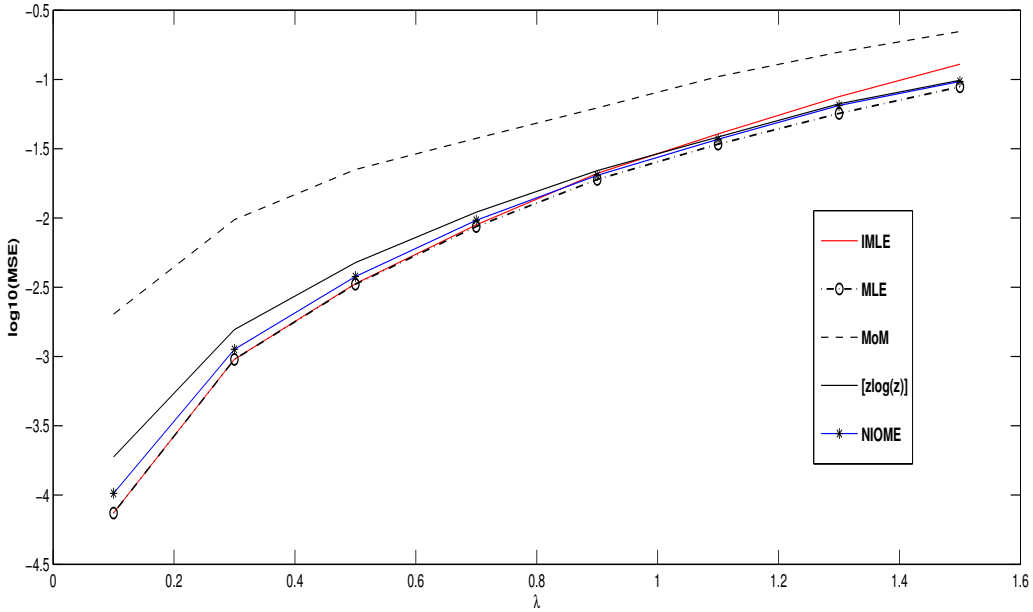

Figure 3.9: MSE estimates of the shape parameter λ of the CIG clutter.

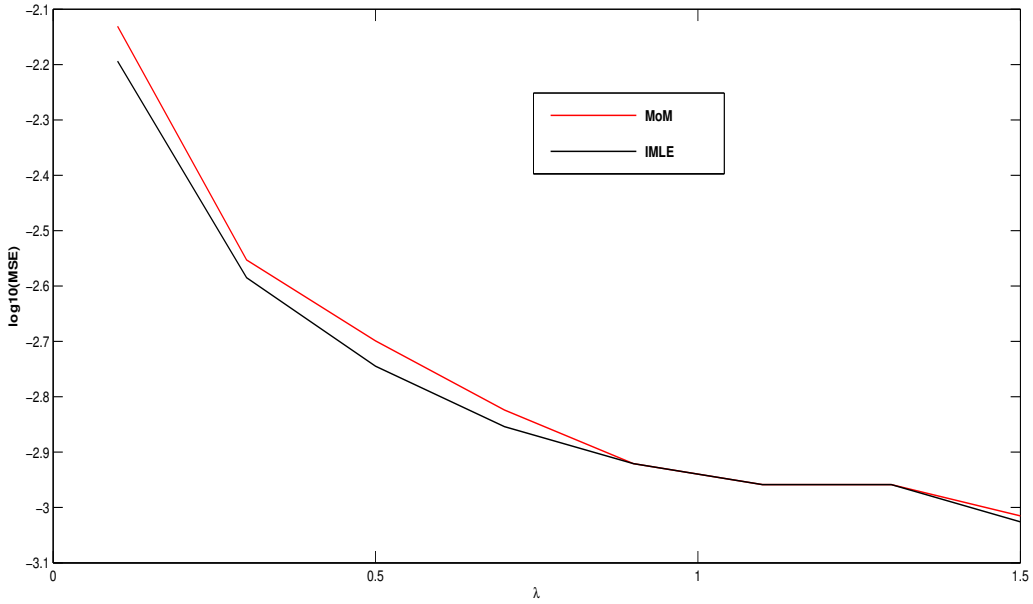

Figure 3.10: MSE estimates of the mean parameter μ of the CIG clutter.

For $\mu = 0.9$, λ varies from 0.1 to 1.5 with a step equal to 0.2 and the number of samples $M = 1000$.

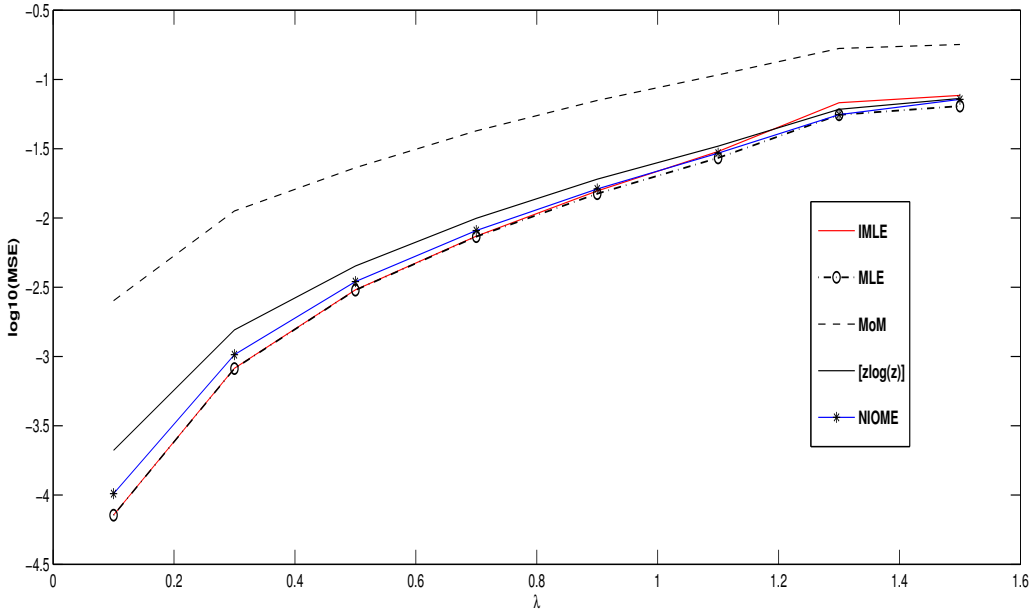

Figure 3.11: MSE estimates of the shape parameter λ of the CIG clutter.

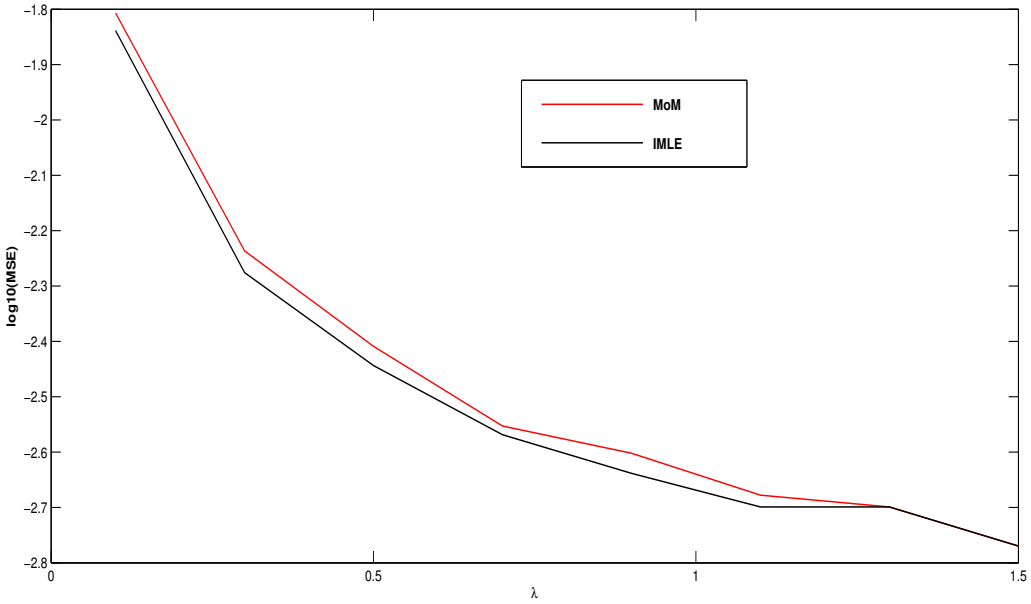

Figure 3.12: MSE estimates of the mean parameter μ of the CIG clutter.

From figures (3.5,3.7,3.9,3.11), we observe that the IMLE has comparable performance compared to the MLE and out performs all the other estimator methods where it has a lowest MSE for different values of μ and at the same time we observe that the IMLE method requires lower computation time than the MLE method.
Figure (3.6,3.8,3.10,3.12) present the comparison of the of the IMLE and the HOME estimation methods for the parameter μ and different values of λ . We observe that, the IMLE method improves the accuracy of estimation compared to the HOME method.

Table 3.2: Computing mean time in seconds to estimate the shape parameter of IG-CG using IMLE and MLE estimators for different values of μ

λ	μ	$T_{IMLE}(s)$	$T_{MLE}(s)$
[0.1 : 0.2 : 1.5]	0.3	0.0294	0.0404
[0.1 : 0.2 : 1.5]	0.5	0.0356	0.0406
[0.1 : 0.2 : 1.5]	0.7	0.0337	0.0405
[0.1 : 0.2 : 1.5]	0.9	0.0328	0.0394
[0.1 : 0.2 : 1.5]	1	0.0352	0.0430

Table 3.2 represents the mean of computational time of IMLE and MLE for different values of μ to estimate λ which varies from 0.1 to 1.5 with step equal 0.2 and M=1000 . we calculated the mean of computational time and we compared between them , we observe that the mean of T_{IMLE} has the lowest mean time compared to the T_{MLE}.

3.8 Conclusion

An iterative maximum likelihood estimation method has been proposed to estimate the shape and the mean parameters of the CIG distributed clutter. The simulation results indicate that the proposed IMLE method has comparable estimation accuracy as the MLE method but with a gain in processing time for the shape parameter. Also, this method improves the estimation accuracy of the mean parameter.

Chapter 4

A Bayesian CFAR Detector in Pearson distributed clutter in homogeneous and non-homogeneous environment

Contents

Abstract

In this chapter, we analyze the performance of the Bayesian predictive inference approach in homogeneous and non homogeneous clutter modeled by a Pearson V distribution, the non-homogeneity is modeled as a step function discontinuity in the reference cells. The target in the CUT is assumed to fluctuate according to the Swerling I, this method can output such detectors with the constant false alarm rate (CFAR) property, we calculated the probability of false alarm (Pfa) and probability of detection (Pd) using this method then we compared pd Bayesian with other detectors are cell average of constant false alarm rate (CA-CFAR) and the Greatest of (GO-CFAR) and Smallest of (SO-CFAR) in homogeneous clutter. The obtained results showed that the best Pd performance is obtained by Bayesian Predictive Approach. In non homogenous clutter, we compared the ordered statistic CFAR (OS-CFAR) with Bayesian CFAR. The results showed that the Bayesian CFAR provides the Pd performance and it is robust against strong interferences.

4.1 Introduction

In radar detection prediction, the clutter level highly affects detection performances, in terms of probability of detection and probability of false alarm rate. Constant false alarm rate (CFAR) detection refers to a common form of adaptive algorithm used in radar systems to detect target returns against a background of noise, clutter and interferences. Many works have been proposed to guarantee the CFAR property employing techniques in homogeneous and no-homogeneous environments [2, 3, 4]. In radar automatic detection, the signal received is sampled in range by the range resolution cells. The clutter background in the CUT is estimated by averaging the outputs of the nearby resolution cells. The detection threshold is obtained by scaling the noise level estimate with a constant to achieve a desired Pfa, this is the conventional (CA-CFAR) detector proposed by Finn and Johnson [2]. In the Greatest-of Constant false alarm rate (GO-CFAR) [3], the leading and lagging reference cells are separately summed and the larger of the two is used to set a threshold. In the Smallest-of constant false alarm rate (SO-CFAR) [3], the smallest is used to set the threshold. In non-homogeneous clutter, the Ordered Statistic CFAR (0S-CFAR) was proposed in [4] to deal with the presence of interfering targets. This chapter proposes to use the Bayesian predictive approach in a clutter modeled by Pearson V distribution in homogeneous and non-homogeneous situations. This method yields a detector with the CFAR property which is used to construct the Bayesian predictive distribution of the CUT given the reference cells [23]. The Bayesian approach was proposed to develop univariate clutter models which is clarified with the particular case for exponentially distributed clutter, then this method is extended to two parameter clutter models to analyze the performance of Bayesian CFAR detector in homogeneous and non-homogeneous clutter modeled by a Pareto type 2 and Weibull distributed clutter [24, 25]. In this chapter, we propose a Bayesian CFAR detector in clutter modeled by a Pearson V distribution. We derive Pfa and we prove that this detector is CFAR with respect to the dispersion parameter. Then, we assess Pd using an appropriate test statistic in homogenous clutter and we compare the detection performance with that of the CA-CFAR, the GO-CFAR and the SO-CFAR [26, 27]. In non-homogeneous clutter, we incorporate some interfering targets in some of the reference cells and we compared the performance with that of the OS-CFAR detector [27, 28]. The robustness of the proposed detector is then studied in terms of the Pfa regulation and Pd.

4.2 CFAR detection

In practical radar detection systems, the problem is to automatically detect a target in thermal noise plus clutter. Several methods were proposed to detect it such as Constant False Alarm Rate (CFAR) detection which refers to a common form of adaptive algorithm used in radar systems to detect target returns against a background of thermal noise, clutter and interference. Radar is an electromagnetic system that detects, locates, and recognizes target

objects. Radar transmits electromagnetic signal and then receives echoes from target objects to get their location or other information. The received signal is frequently corrupted by noise and clutter. The disturbances may cause serious performance issues with radar systems by concluding these signals as targets. To make a right censoring decision, the receiver is desired to achieve a constant false alarm rate (CFAR) and a maximum probability of target detection. Modern radars usually detect targets by comparing with adaptive thresholds based on a CFAR processor. In this processor, the threshold is determined dynamically based on the local background noise/clutter power. The CFAR detectors have been widely used in radar signal processing applications to detect the targets from noisy background.

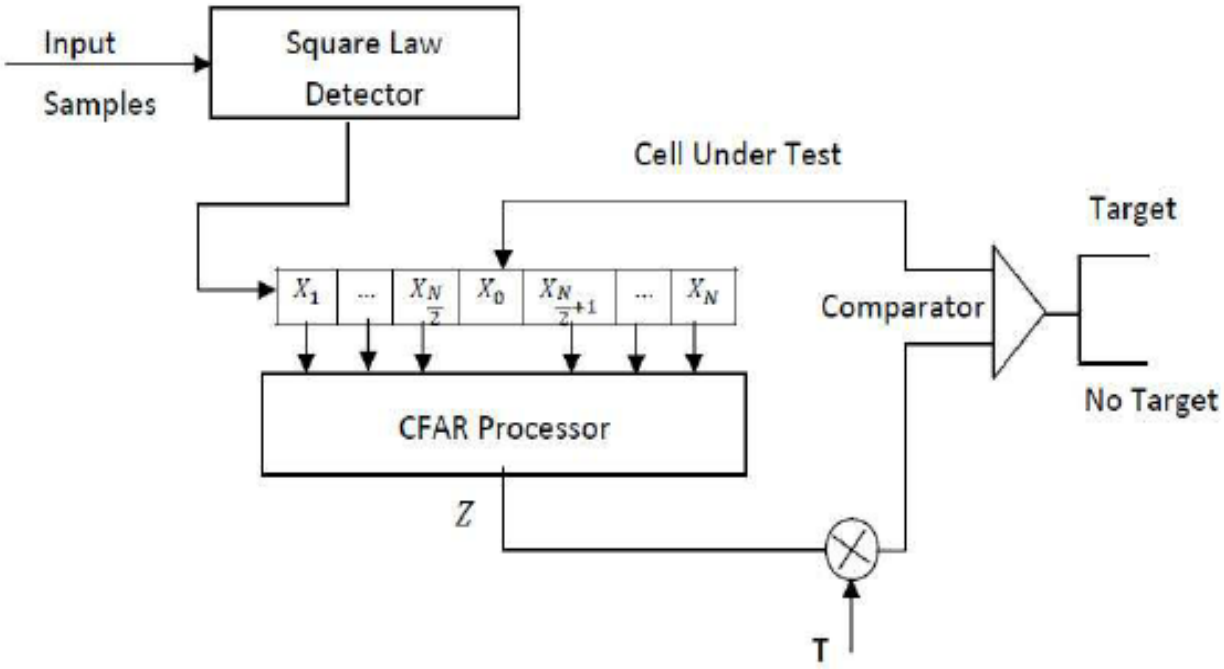

Figure 4.1: Bloc diagram of a typical CFAR detector.

The CA-CFAR [2], GO-CFAR, SO-CFAR [3] and OS-CFAR [4] following are the most used and have been proposed to detect target with high precision.
In all CFAR methods, a training window around the cell under test is selected with which the noise plus interference power level is estimated. Indeed, some cells around the cell under test are ignored so that a wideband target or clutter can be detected or removed. These cells are illustrated in the following Figure.

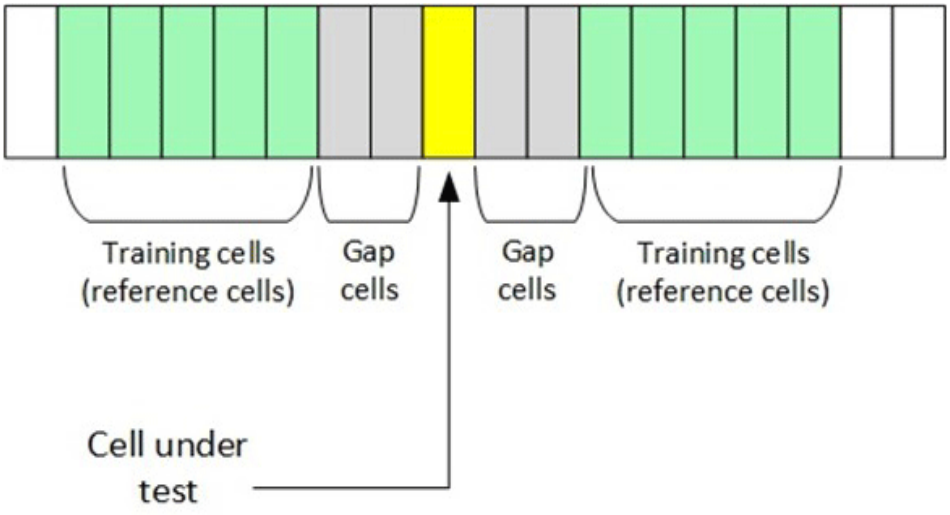

Figure 4.2: Bloc diagram of reference cells of CFAR detector.

4.2.1 CA-CFAR detector

The Cell averaging CFAR (CA-CFAR) is optimum for a uniform background noise and clutters. For instance, if the sensor is in a dense scattering environment such as on a forest with a dense trees population, the CA-CFAR can be used to find an optimum threshold for the power profile. However, this algorithm fails in keeping the false alarm rate constant in the presence of non-uniform clutters. In fact, for computing the threshold value, the noise plus clutter power is estimated by the summation of the cell reference values and denoting it as

$$Z = \sum_{i=1}^{N} X_i \tag{4.1}$$

Where $X_1,\ X_2, \ldots X_N$ are IID .
The Z value should be multiplied to a constant T to maintain the desired Pfa.

$$T = (Pfa)^{-\frac{1}{N}} - 1 \tag{4.2}$$

Where N is the length of the reference window and Pfa is the false alarm probability, which is defined as:

$$Pfa = Pr(X_0 \geq T/H_0) \tag{4.3}$$

The probability of detection under hypothesis H_1 is defined as:

$$Pd = Pr(X_0 \geq T/H_1) \tag{4.4}$$

Where H_1 represents the hypothesis of the presence of a target.

4.2.2 GO-CFAR detector

This configuration uses the greater of (GO) the mean level estimates either side of the CUT. Similar estimates can be made of the losses associated with other CA variants. For the GO-CFAR, the threshold is formed using the greater of the two CA-CFAR regions either side of the cell under test. In this detector Z is

$$Z = \max(Y_1, Y_2) \tag{4.5}$$

4.2.3 Smaller of CFAR (SO-CFAR)

This configuration uses the smaller of (SO) the mean level estimates either side of the cell under test. It is able to resolve closely spaced targets but gives a high false alarm rate around clutter edges.So, Z is

$$Z = \min(Y_1, Y_2) \tag{4.6}$$

4.2.4 Ordered Statistic (OS-CFAR)

In an ordered statistics OS-CFAR, the X range cells in the reference cells window (X(1), X(2), ... , X(N)) are ranked according to magnitude to give ordered samples, X(1) < X(2) <. . . < X(N). The noise power is estimated from the magnitude of the kth largest cell. The optimum value of k^{th} is found to be around 3N/4.
More details about variants of CFAR detectors can be found in [2, 3, 4, 29]

4.3 Problem formulation

In CFAR detectors in general, the received signal is sampled in distance.The samples are sent to a shift register of length N forming the reference window.The data available in the window of the reference are used to obtain an estimate Z of the power of the clutter.This estimate is multiplied by a factor T making it possible to maintain the constant false alarm probability under the Neyman-Pearson criterion. The presence of a target or its absence is obtained by comparison of the content of the CUT with the T.Z adaptive threshold. The CUT Q_0 from the center tap is compared with an adaptive threshold to make a decision about the presence (H_1) or the absence (H_0) of a target in the CUT.

$$Q_O \underset{H_0}{\overset{H_1}{\gtrless}} T.Z \tag{4.7}$$

Figure 4.3 shows the block diagram of CFAR detectors in homogeneous clutter; namely the CA-CFAR, SO-CFAR and GO-CFAR.
In radar detection problem, we always search for methods that give better performance than the classical approach of the CFAR detectors based on Neyman-Pearson criteria.
In order to address this question, we formulate the detection problem in terms of the Bayesian predictive distribution; the reason for this is that it creates the distribution of the CUT conditioned on the reference cells. This chapter deals the detection performance of the Bayesian CFAR detector compared with CA, SO, and GO-CFAR detector in homogeneous and non-homogeneous spiky clutter distributed according to Pearson V. In a homogeneous background, we assume that the reference range samples $Q_1 Q_2 \ldots Q_N$ are IID and follow the Pearson V distribution [29] with a pdf

$$P_Q(q_i) = \frac{\gamma}{\sqrt{2\pi}} \frac{1}{{q_i}^{\frac{3}{2}}} e^{\frac{-\gamma^2}{q_i}} \qquad i = 1, 2, \ldots N \tag{4.8}$$

Where γ is the dispersion or scale parameter of the distribution. In non-homogeneous case, we assume that the reference cells samples are independent but not identically distributed.
The Bayesian detector can be written as [24]

$$Q_0 \backslash Q_1 \ldots\ldots Q_N \underset{H_0}{\overset{H_1}{\gtrless}} \tau \tag{4.9}$$

Where $Q_0 \backslash Q_1 \ldots\ldots Q_N$ is the Bayesian predictive distribution of the CUT, conditioned on the reference cells, and τ is the threshold.
The next section presents and describes the Bayesian approach and the way of deriving Pfa.

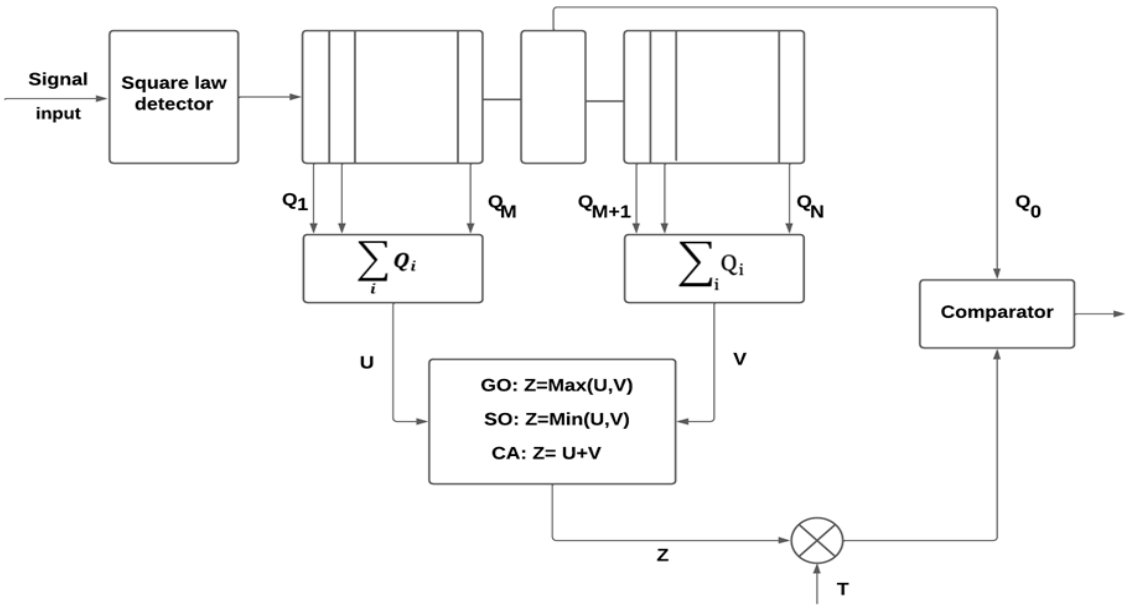

Figure 4.3: Block diagram of the CA, GO and SO-CFAR detectors.

4.4 The Bayesian approach

Bayesian approach is performed by combining the prior information and the sample information into what is called the posterior distribution, from all decision and inferences are made [23] which create the bayesian predictive distribution of CUT given the references cells that is $Q_0 \backslash Q_1, Q_2 ..... Q_N$ [24], the form of the test is:

$$Q_0 \backslash \{Q_1 = q_1 ..... Q_N = q_N\} \gtrless_{H_0}^{H_1} \tau \tag{4.10}$$

Where $\tau > 0$ is to be determined via an expression for the Pfa, the expression for the Pfa is given by:

$$Pfa = Pr\left(Q_0 > \tau \backslash Q_1 = q_1 ..... Q_N = q_N\right) \tag{4.11}$$

$$= \int_{\tau}^{\infty} f_{Q_0 \backslash Q_1 ... Q_N (q_0 \backslash q_1 ... q_N)} dq_0 \tag{4.12}$$

Where $f_{Q_0 \backslash Q_1 ... Q_N (q_0 \backslash q_1 ... q_N)}$ is the density of the predictive distribution. (4.12) provides a general expression for the Pfa for the Bayesian test (4.10) for one parameter clutter models as in Pearson V distributed clutter, the reference cells are modeled with density (4.8) this is used to demonstrate how appropriate prior distribution for γ can be selected [24].

To determine this we can construct the Jeffreys prior [30] which is based on the Fisher information matrix.
The next section presents the way of calculating the Fisher information matrix and how we obtain the Pfa of the Bayesian CFAR detector.

4.5 The Bayesian Approach of Pearson V clutter

In this section, we calculate Pfa and the Bayesian CFAR detector. For that we need to follow these steps:
The logarithm of the pdf (4.8) is

$$log f_Q(q) = log\gamma - log\sqrt{2\pi} - logq^{\frac{3}{2}} - \frac{\gamma^2}{2q} \tag{4.13}$$

And,

$$\begin{aligned} \frac{d^2 log f_Q(q)}{d\gamma} &= \frac{-1}{\gamma^2} - \frac{1}{q_i} \\ &= -\left[\frac{1}{\gamma^2} + \frac{1}{q_i}\right] \\ &= -E\left[\frac{1}{\gamma^2} + \frac{1}{q_i}\right] \\ &= \frac{1}{\gamma^2} + E\left[q^{-1}\right] \\ &= \frac{1}{\gamma^2} + \int_0^\infty q^{-1} f_Q(q)\, dq \end{aligned} \tag{4.14}$$

So,

$$\frac{d^2 log f_Q(q)}{d\gamma} = \frac{2}{\gamma^2} \tag{4.15}$$

Where (4.15) is also the mean of order -1 of the Pearson V distribution . The fisher information matrix for distribution with pdf (4.8) is the singleton given by

$$F = \left[\frac{2}{\gamma^2}\right] \tag{4.16}$$

The Jeffreys prior of the Fisher information matrix is proportional to:

$$\sqrt{detE} = \sqrt{\frac{2}{\gamma^2}} = \frac{\sqrt{2}}{\gamma} \tag{4.17}$$

For a series of IID Pearson V clutter (4.8),the joint density of the window cells is :

$$f_{Q_1,Q_2.....Q_N\backslash\gamma}(q_1 q_2.....q_N\backslash\gamma) = \frac{\gamma^N}{(2\pi)^N} \prod_{i=1}^{N} (q)^{\frac{3}{2}} e^{-\gamma^2 \sum_{i=1}^{N} \frac{1}{2q_i}} \tag{4.18}$$

The joint density of the Pearson parameter σ, conditioned on the reference cells using the Bayes theorem is given by:

$$f_{\gamma\backslash Q_1,Q_2.....Q_N}(\gamma\backslash q_1 q_2.....q_N) = \frac{\frac{\gamma^N}{(2\pi)^N}\prod_{i=1}^{N}(q)^{\frac{3}{2}}\, e^{-\gamma^2\sum_{i=1}^{N}\frac{1}{2q_i}}}{\int_0^\infty \frac{\gamma^N}{(2\pi)^N}\prod_{i=1}^{N}(q)^{\frac{3}{2}}\, e^{-\gamma^2\sum_{i=1}^{N}\frac{1}{2q_i}}\frac{\sqrt{2}}{\gamma}d\gamma} \tag{4.19}$$

$$= \frac{\gamma^N e^{-\gamma^2\sum_{i=1}^{N}\frac{1}{2q_i}}\left(\sum_{i=1}^{N}\frac{1}{2q_i}\right)^{\frac{N}{2}}}{\frac{\sqrt{2}}{2}\Gamma\left(\frac{N}{2}\right)} \tag{4.20}$$

The CUT has an Pearson V distribution with dispersion parameter γ the predictive distribution under H_0 is given by: Where (4.20) has been used

$$f_{Q_0\backslash Q_1,Q_2.....Q_N(q_0\backslash q_1,q_2.....q_N)} = \int_0^\infty \frac{\gamma}{\sqrt{2\pi}}\left(\frac{1}{q_0}\right)^{\frac{3}{2}} e^{-\gamma^2\frac{1}{2q_0}}\frac{\gamma^N e^{-\gamma^2\sum_{i=1}^{N}\frac{1}{2q_i}}\left(\sum_{i=1}^{N}\frac{1}{2q_i}\right)^{\frac{N}{2}}}{\frac{\sqrt{2}}{2}\Gamma\left(\frac{N}{2}\right)}\frac{\sqrt{2}}{\gamma}d\gamma \tag{4.21}$$

$$= \frac{\left(\sum_{i=1}^{N}\frac{1}{2q_i}\right)^{\frac{N}{2}}\Gamma\left(\frac{N+1}{2}\right)}{\sqrt{2\pi}\,(q_0)^{\frac{3}{2}}\Gamma\left(\frac{N}{2}\right)\left[\frac{1}{q_0}+\sum_{i=1}^{N}\frac{1}{2q_i}\right]^{\frac{N+1}{2}}} \tag{4.22}$$

We used the density (4.22) under H_0 and we calculated the Pfa in terms of τ we obtained this equation:

$$P(Q_0 > \tau\backslash Q_1, Q_2, ...Q_N) = \int_\tau^\infty f_{Q_0\backslash Q_1,Q_2.....Q_N(q_0\backslash q_1,q_2.....q_N)}dq_0 \tag{4.23}$$

$$Pfa(\tau) = \int_\tau^\infty f_{Q_0\backslash Q_1,Q_2.....Q_N(q_0\backslash q_1,q_2.....q_N)}dq_0 \tag{4.24}$$

$$Pfa(\tau) = \int_\tau^\infty \frac{\left(\sum_{i=1}^{N}\frac{1}{2q_i}\right)^{\frac{N}{2}}\Gamma\left(\frac{N+1}{2}\right)}{\sqrt{2\pi}\,(q_0)^{\frac{3}{2}}\Gamma\left(\frac{N}{2}\right)\left[\frac{1}{q_0}+\sum_{i=1}^{N}\frac{1}{2q_i}\right]^{\frac{N+1}{2}}}dq_0 \tag{4.25}$$

$$Pfa(\tau) = \frac{\left(\sum_{i=1}^{N}\frac{1}{2q_i}\right)^{\frac{N}{2}}\Gamma\left(\frac{N+1}{2}\right)}{\sqrt{2\pi}\Gamma\left(\frac{N}{2}\right)}\int_\tau^\infty \frac{1}{(q_0)^{\frac{3}{2}}\left[\frac{1}{2q_0}+\sum_{i=1}^{N}\frac{1}{2q_i}\right]^{\frac{N+1}{2}}}dq_0 \tag{4.26}$$

We solve Pfa as a function of τ numerically. When τ decreases, we observe that Pfa increases to approach 1, and when τ increases, Pfa decreases to approach 0. In addition, if we change the value of the scale parameter, we observed that Pfa remains constant which proves that this Bayesian detector has the CFAR property. Then we calculated the Pd using monte carlo simulation the test of this detector is

$$Pfa(\tau) < Pfa \tag{4.27}$$

Which is equivalent to $CUT > \tau$
Then, the test statistics is

$$Pfa(CUT) \underset{H_0}{\overset{H_1}{\gtrless}} Pfa \tag{4.28}$$

4.6 Results and discussion

This section presents the performance of the Bayesian CFAR detector in homogeneous and non-homogeneous clutter. Based on (4.28), it will compared to the CA-CFAR, SO-CFAR and GO-CFAR detectors [26, 27]. Where from [26, 27]., the Pd of these detectors is given by:

$$Pd^{CA} = e^{-\frac{\gamma}{\sigma}\sqrt{NT}} \tag{4.29}$$

$$Pd^{GO} = 2\sqrt{\frac{2M}{\pi}} \int_0^{\infty} e^{-\frac{T\gamma^2}{2y^2\sigma^2}} Erfc\left[\frac{y\sqrt{M}}{\sqrt{2}}\right] e^{-\frac{My^2}{2}} dy \tag{4.30}$$

$$pd^{SO} = 2\sqrt{\frac{2M}{\pi}} \int_0^{\infty} e^{-\frac{T\gamma^2}{2y^2\sigma^2}} Erf\left[\frac{y\sqrt{M}}{\sqrt{2}}\right] e^{-\frac{My^2}{2}} dy \tag{4.31}$$

These equations show that Pd is a function of the ratio of the dispersion parameter of the clutter on the variance of the Swerling I model of the target. As in [26, 27] the authors define the generalized signal-to-noise ratio (Generalized SNR) as

$$GSNR = 20log\left(\frac{\sigma}{\gamma}\right) \tag{4.32}$$

The GSNR ratio should not be considered a signal-to-noise ratio because the second order moment for the Pearson V distribution is infinite [29].
To find the value of σ (the power of clutter) we have

$$\frac{q}{2\sigma^2} = \frac{1}{\mu} \tag{4.33}$$

So,

$$\sigma = \sqrt{\frac{\mu}{2}} \tag{4.34}$$

We substituted (4.34) into (4.32), finally we found

$$GSNR = 20log\left(\frac{\sqrt{\frac{\mu}{2}}}{\gamma}\right) \tag{4.35}$$

$$\mu = \left(10^{\frac{GSNR}{20}} \times \gamma\sqrt{2}\right)^{\frac{1}{0.5}} \tag{4.36}$$

4.6.1 Homogenous clutter

To illustrate the performance of the Bayesian CFAR detector considered in a homogeneous situation, we plot Pd of the proposed Bayesian CFAR detector and the CA-CFAR,SO-CFAR and GO-CFAR detectors as a function of the GSNR for a desired $Pfa = 10^{-3}$, $\gamma = 0.5$ and $\gamma = 2$.

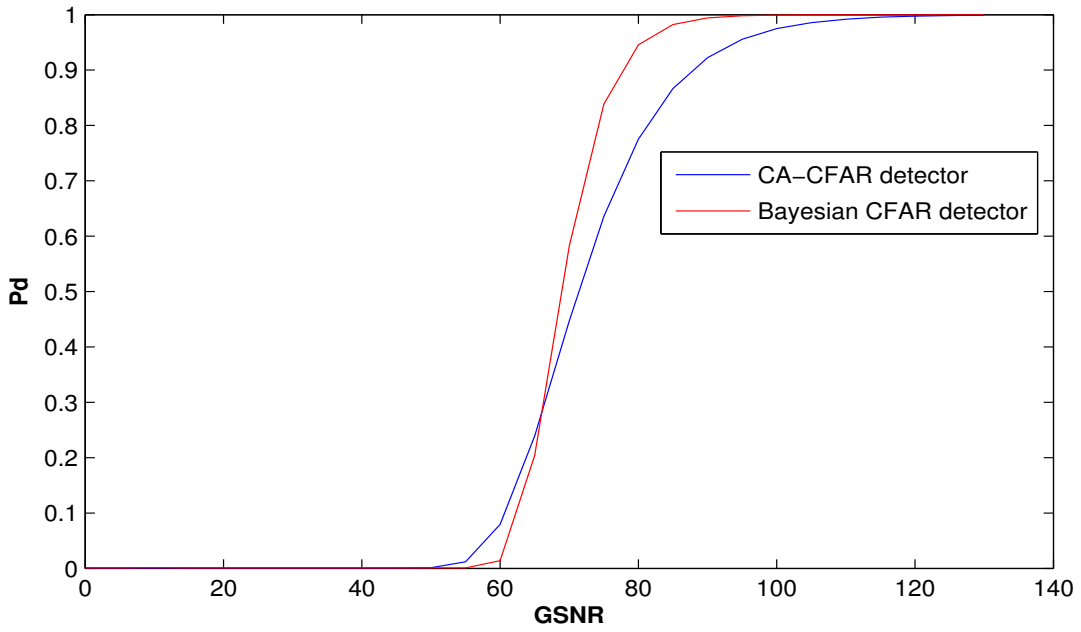

Figure 4.4: Detection performance of the proposed Bayesian CFAR detector and CA-CFAR detectors in homogeneous clutter where N=16, $\gamma = 0.5$ and $Pfa = 10^{-3}$

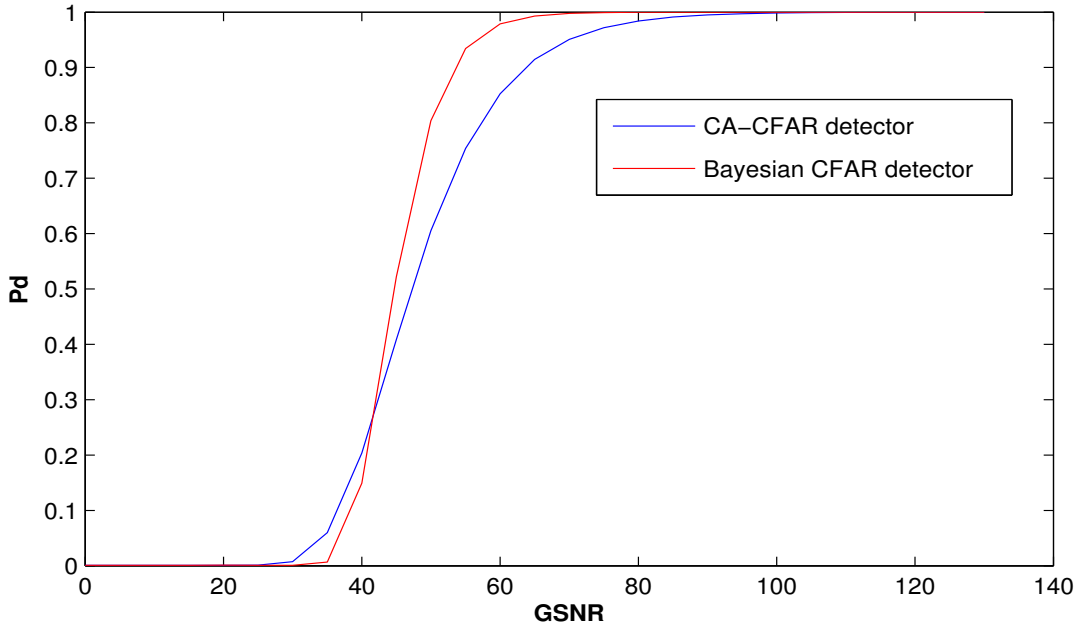

Figure 4.5: Detection performance of the proposed Bayesian CFAR detector and CA-CFAR detectors in homogeneous clutter where N=16, $\gamma = 2$ and $Pfa = 10^{-3}$

Figs (4.4) and (4.5) present the performance detection of the Bayesian CFAR and CA-CFAR detectors when$\gamma = 0.5$ and $\gamma = 2$ .We observe from figure (4.4) that the detection performance of the Bayesian CFAR detector is better than that of the CA-CFAR detector for GSNR values greater than 70 dB whereas in figure (4.5), the same pattern is observed but for GSNR values greater than 40 dB.

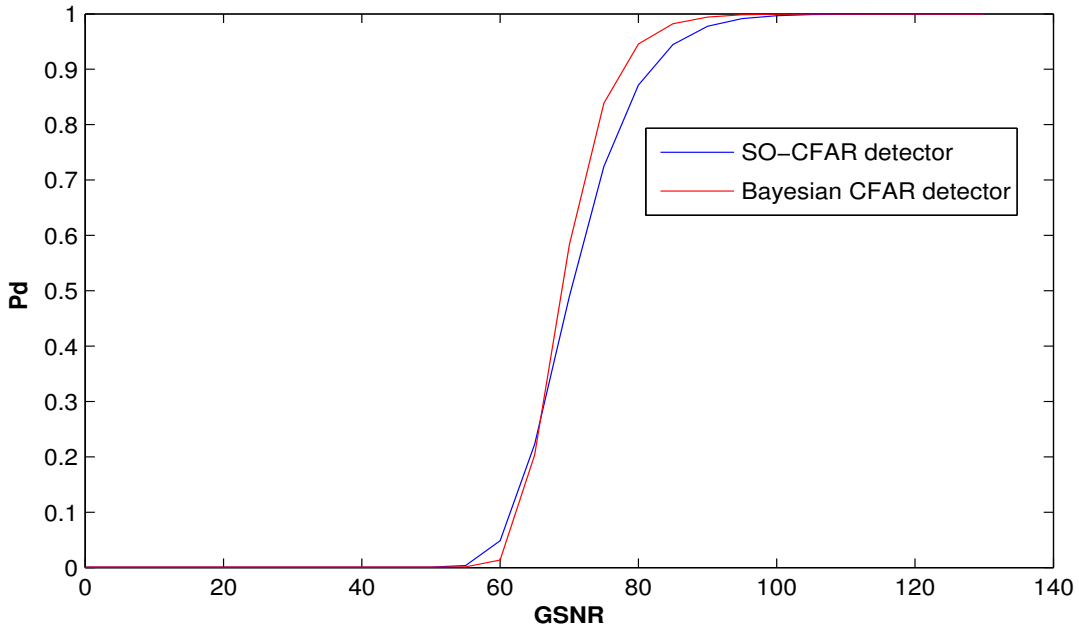

Figure 4.6: Detection performance of the proposed Bayesian CFAR detector and SO-CFAR detectors in homogeneous clutter where N=16, $\gamma = 0.5$ and $Pfa = 10^{-3}$

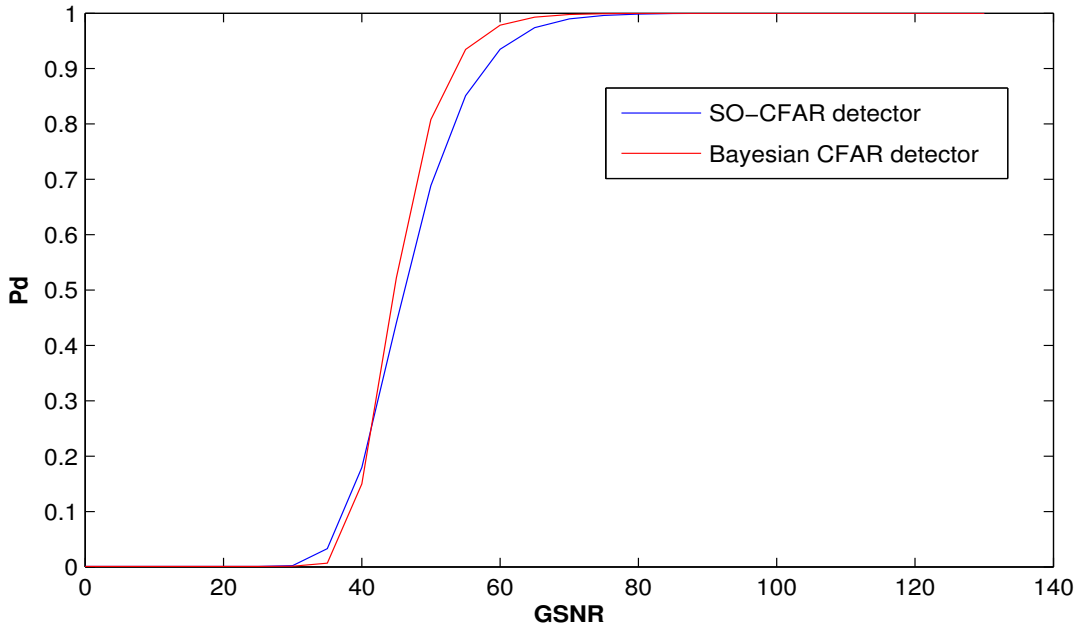

Figure 4.7: Detection performance of the proposed Bayesian CFAR detector and SO-CFAR detectors in homogeneous clutter where N=16, $\gamma = 2$ and $Pfa = 10^{-3}$

Figures (4.6) and (4.7) present the performance detection of the Bayesian CFAR and the SO-CFAR detectors when $\gamma = 0.5$,$\gamma = 2$ respectively. The results show that the Bayesian detector is better for GSNR values greater than 70 db where $\gamma = 0.5$, for $\gamma = 2$, the detection performance is better when the GSNR values are greater than 60 db.

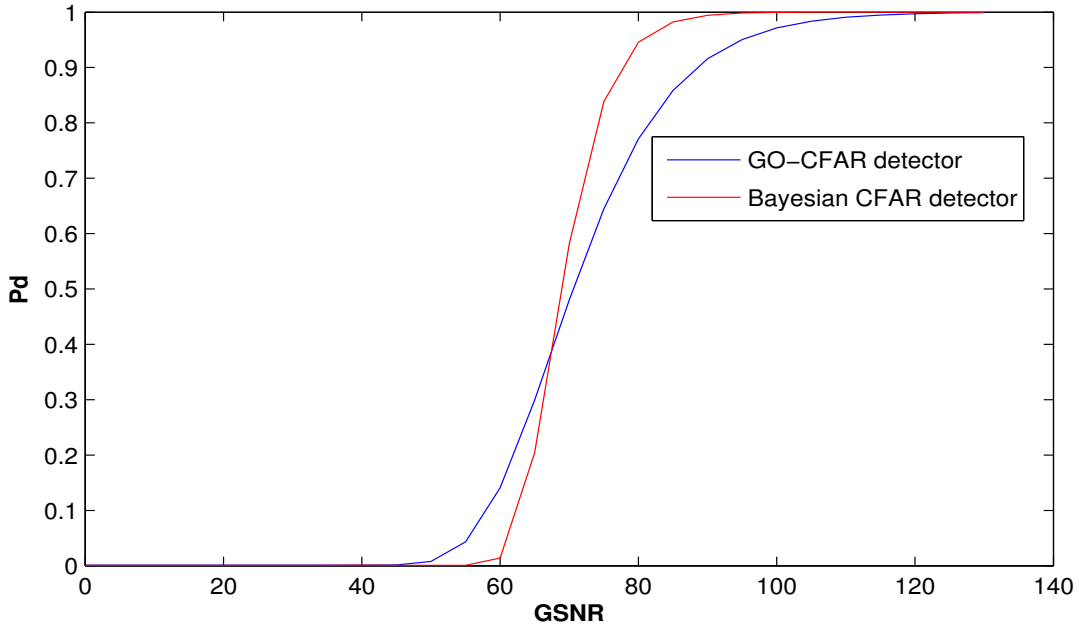

Figure 4.8: Detection performance of the proposed Bayesian CFAR detector and GO-CFAR detectors in homogeneous clutter where N=16, $\gamma = 0.5$ and $Pfa = 10^{-3}$

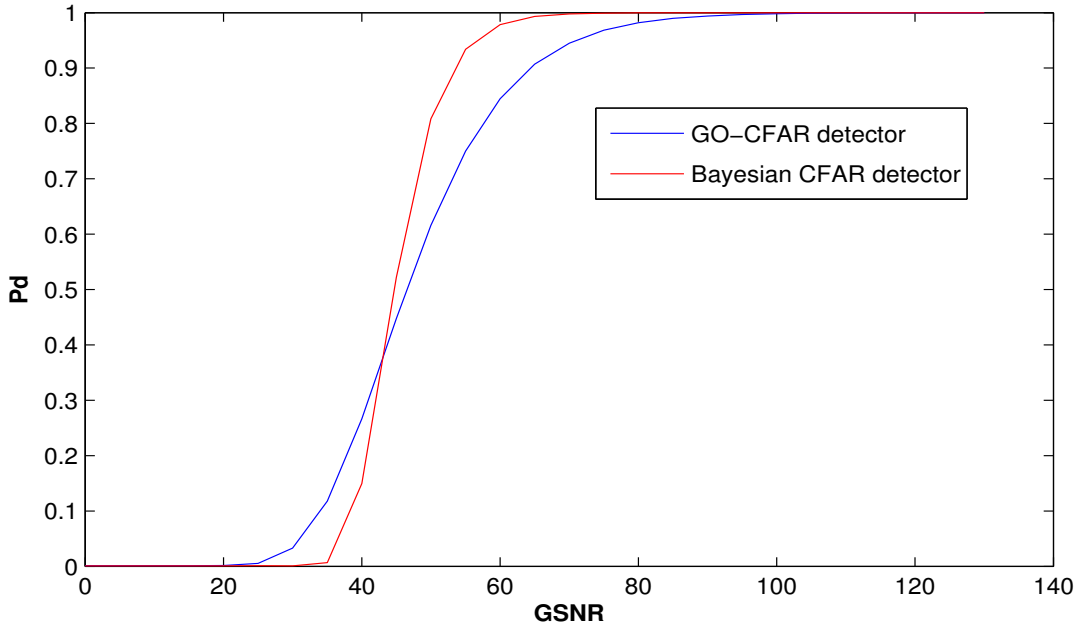

Figure 4.9: Detection performance of the proposed Bayesian CFAR detector and GO-CFAR detectors in homogeneous clutter where N=16, $\gamma = 2$ and $Pfa = 10^{-3}$

Figures (4.8) and (4.9) present the performance of the Bayesian CFAR and GO-CFAR detectors where $\gamma = 0.5$ and $\gamma = 2$. We observe that the detection performance is better for the GSNR values greater than 70 and 60 dB respectively. The comparison between the two detectors shows that the detection performance of Bayesian performance is better than GO-CFAR and from the previous results, we conclude that the scale parameter γ influences the detection performance where Pd increases with γ.

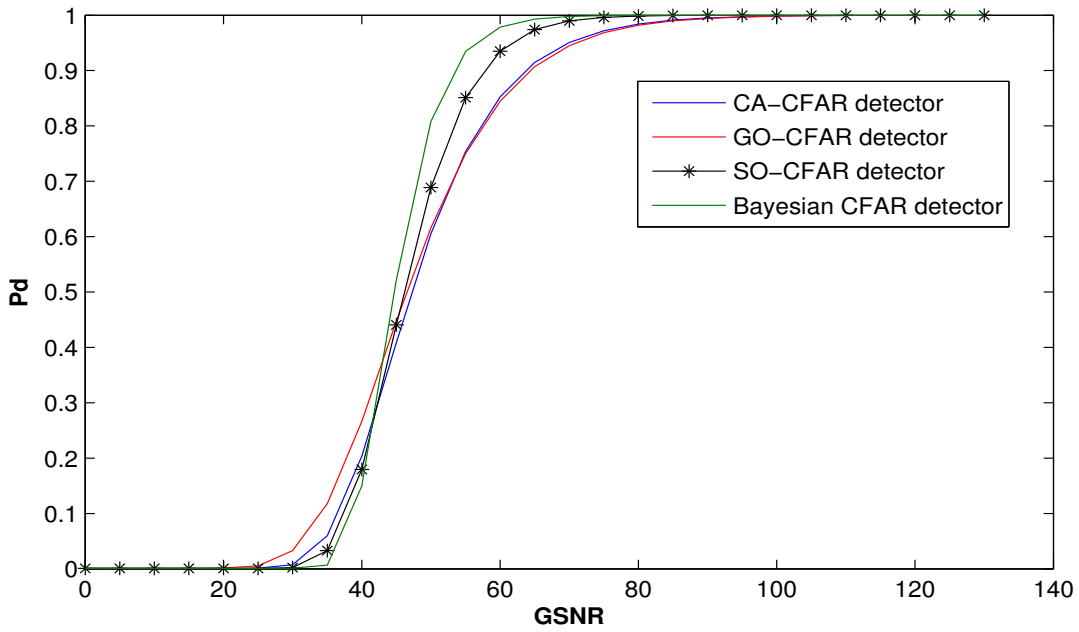

Figure 4.10: Comparison between Bayesian CFAR detector and other detectors in homogeneous clutter where N=16, $\gamma = 2$ and $Pfa = 10^{-3}$

In figure (4.7), we compare the performance of all the previous detectors f for $\gamma = 2$. From this Figure, we observe that the Bayesian CFAR detector has the best detection performance compared with the other detectors especially for high values of the GSNR from 40 dB to 140 dB.

The simulation is carried out for different values of γ, where it is equal 3 and 4 with $Pfa = 10^{-3}$. The results shows that the Pd is related to the dispersion parameter, where the Pd increases with the dispersion parameter increases.

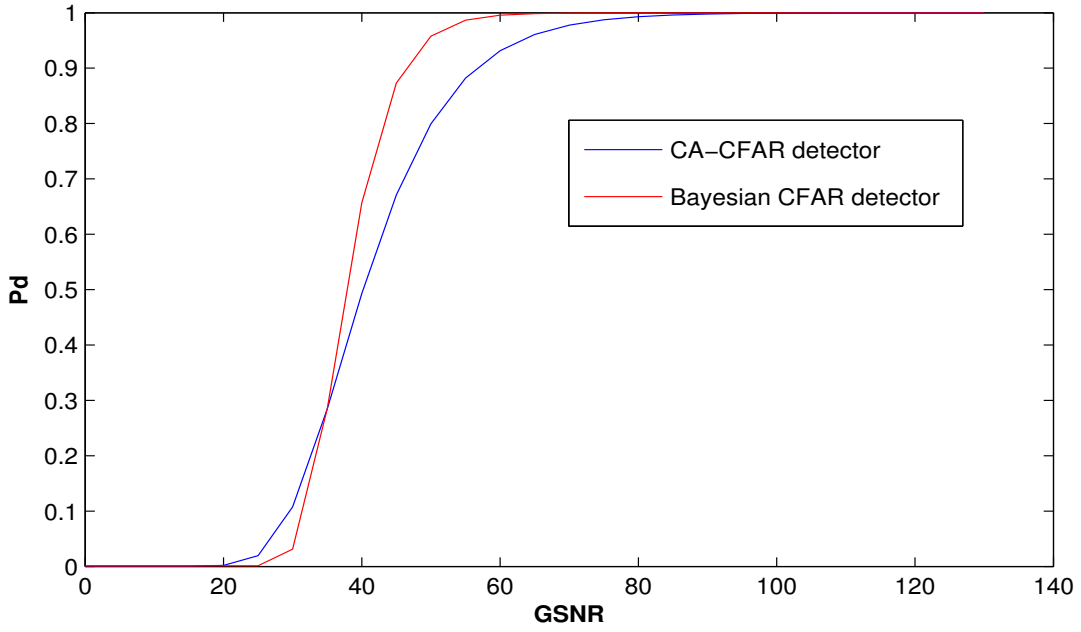

Figure 4.11: Detection performance of the proposed Bayesian CFAR detector and CA-CFAR detectors in homogeneous clutter where N=16, $\gamma = 3$ and $Pfa = 10^{-3}$

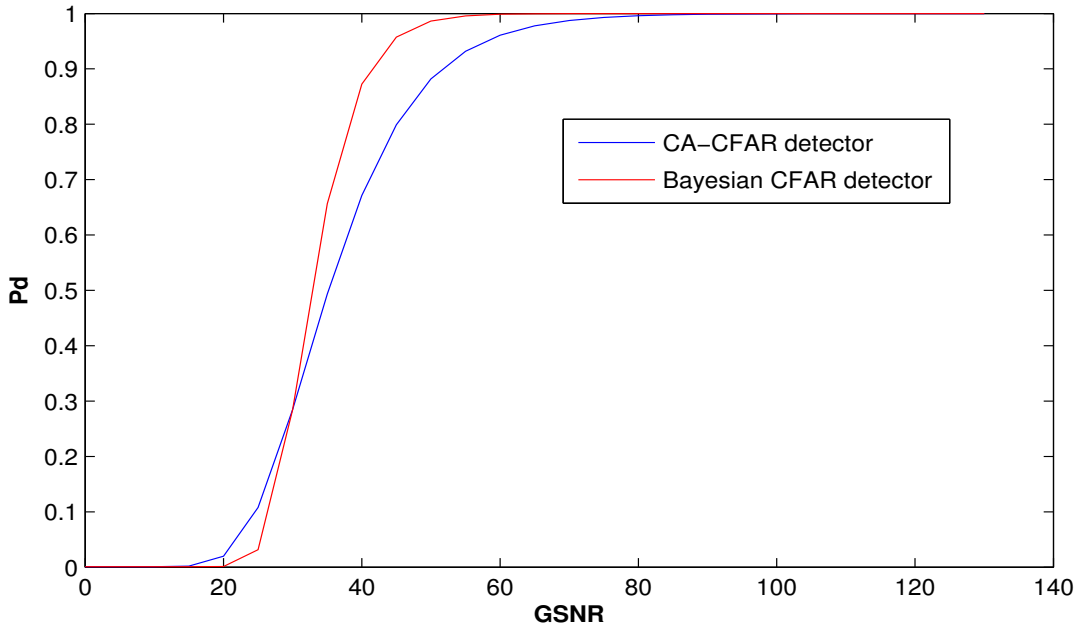

Figure 4.12: Detection performance of the proposed Bayesian CFAR detector and CA-CFAR detectors in homogeneous clutter where N=16, $\gamma = 4$ and $Pfa = 10^{-3}$

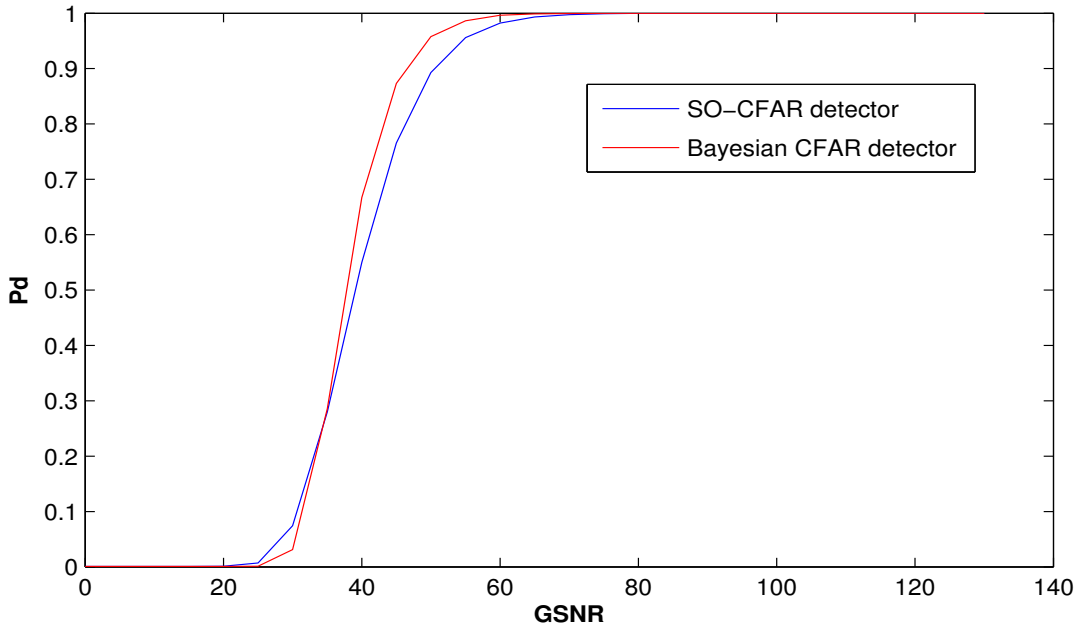

Figure 4.13: Detection performance of the proposed Bayesian CFAR detector and SO-CFAR detectors in homogeneous clutter where N=16, $\gamma = 3$ and $Pfa = 10^{-3}$

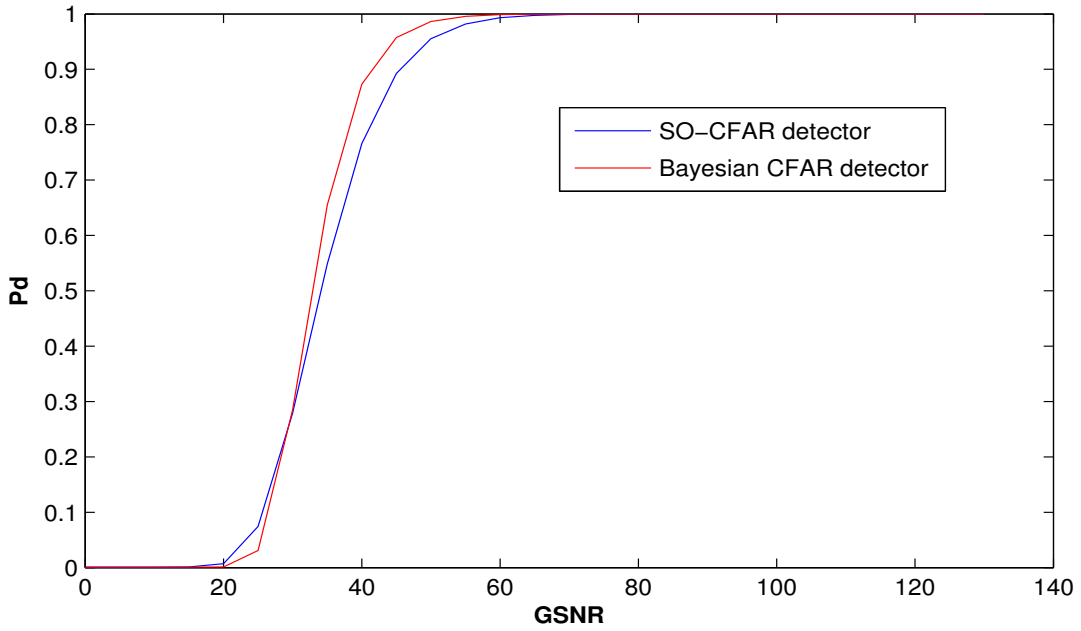

Figure 4.14: Detection performance of the proposed Bayesian CFAR detector and SO-CFAR detectors in homogeneous clutter where N=16, $\gamma = 4$ and $Pfa = 10^{-3}$

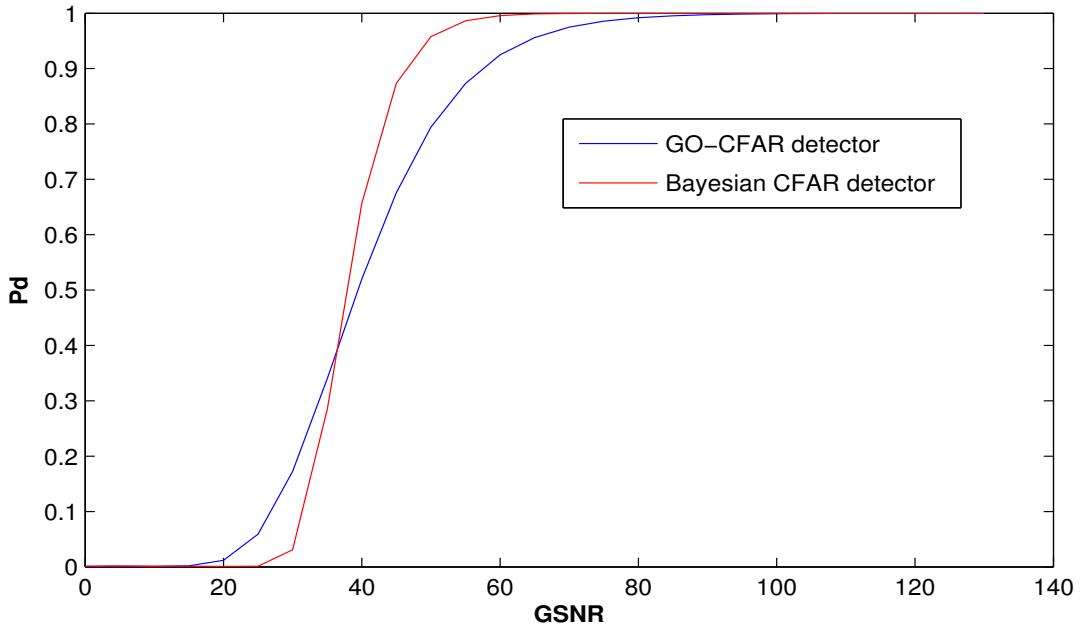

Figure 4.15: Detection performance of the proposed Bayesian CFAR detector and GO-CFAR detectors in homogeneous clutter where N=16, $\gamma = 3$ and $Pfa = 10^{-3}$

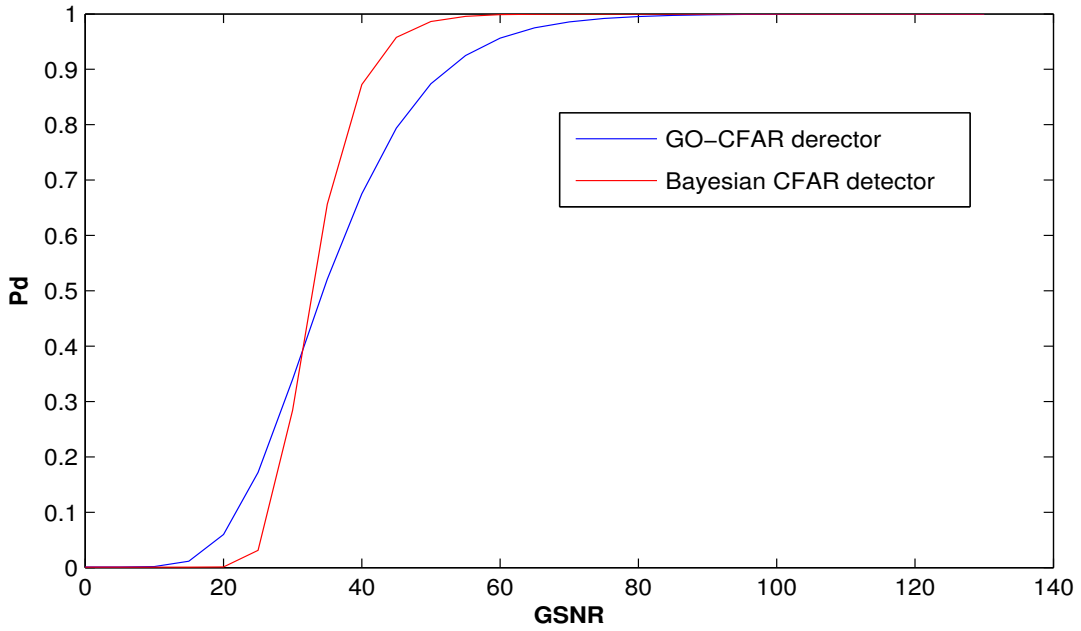

Figure 4.16: Detection performance of the proposed Bayesian CFAR detector and GO-CFAR detectors in homogeneous clutter where N=16, $\gamma = 4$ and $Pfa = 10^{-3}$

4.6.2 Non- homogeneous clutter

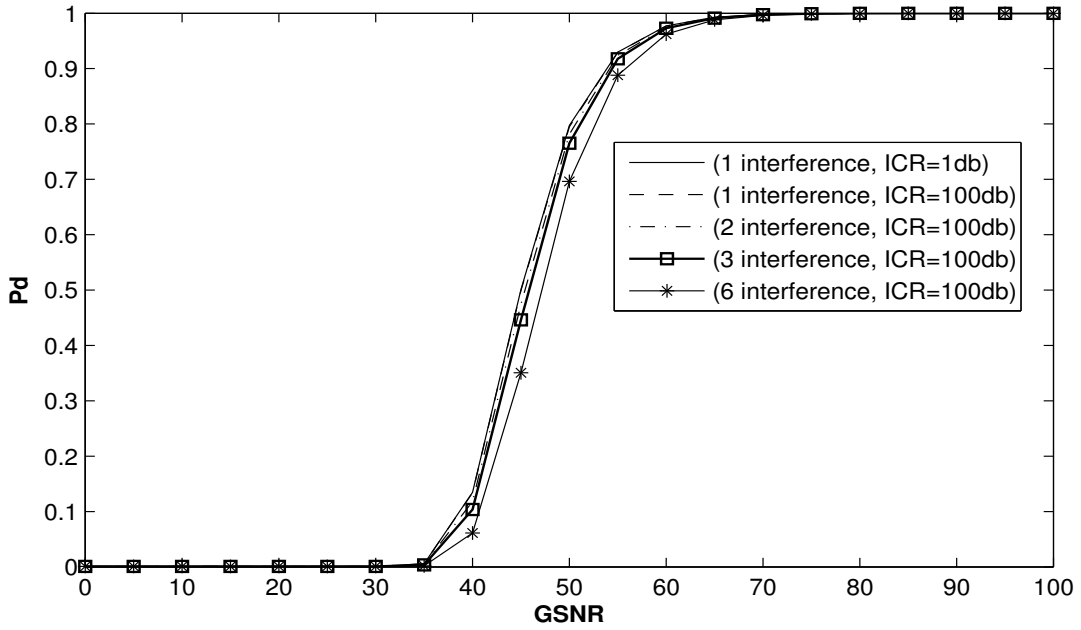

Figure 4.17: Performance of the Bayesian CFAR when the reference cells contains interference where N=16, $\gamma = 2$ and $Pfa = 10^{-3}$

First, figure (4.17) presents the Bayesian CFAR detector in the case where the clutter is non-homogeneous, meaning that there are spurious targets in the reference cells. Figure (4.11) illustrates the performance of this detector when $\gamma = 2$, GSNR=0 to 100 dB, N=16 and a Swerling 1 target is inserted into the reference cells. In the first step, we add one interference with an ICR equal to 1 dB. We observe that the detection performance remains the same as in the case of the absence of interferences. Then we increase the value of the ICR to attain 100 dB. We observe that the detection performance of the Bayesian CFAR detector remains the same as in the case of ICR=1dB. Then, we added two interferences and three interferences with ICR equal to 100 dB. We observe the detection performance decreases slightly. Finally, to check the robustness of this detector, we add six interferences in the reference window with ICR =100 dB. The results show that the performance detection decreases slightly as the level of interferences increases. We also computed Pfa in the case of the presence of interferences and we found the same value around 10^{-3}, we conclude that the Bayesian CFAR detector is robust to strong interferences in the case where the clutter is modeled by a Pearson V distribution.

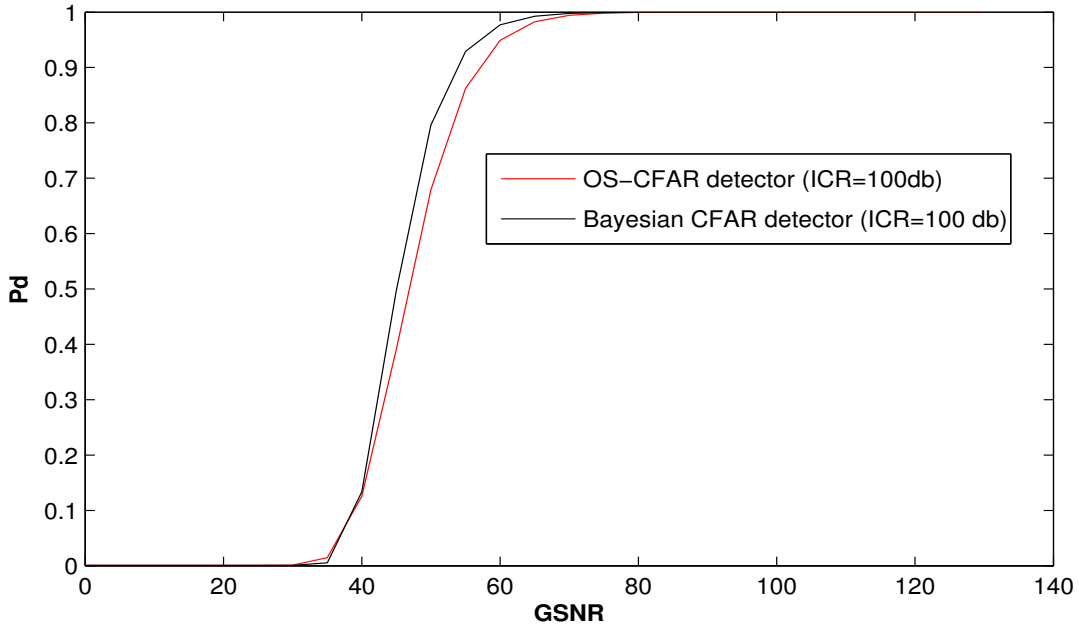

Figure 4.18: Comparison between Bayesian CFAR detector and OS-CFAR detector when the reference cells contains one interference where N=16, $\gamma = 2$ and $Pfa = 10^{-3}$

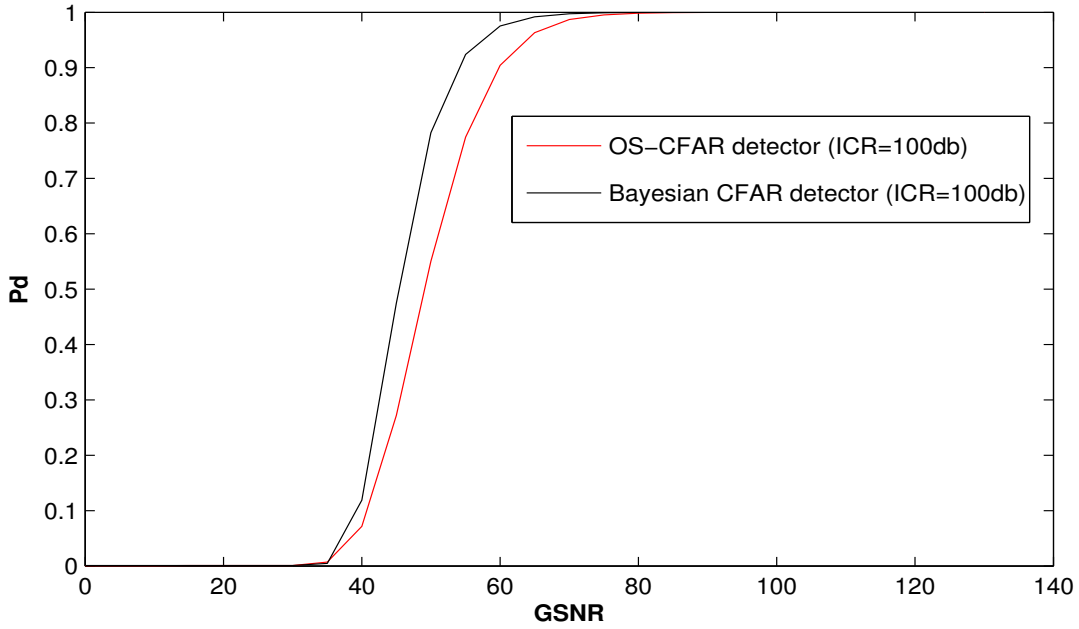

Figure 4.19: Comparison between Bayesian CFAR detector and OS-CFAR detector when the reference cells contains two interference where N=16, $\gamma = 2$ and $Pfa = 10^{-3}$

Next, figures (4.18) and (4.19) present the comparison between Bayesian CFAR and OS-CFAR where $\gamma = 2$, GSNR=0 to 100 dB, N=16.We add one interference in the reference cells where the power of this interference is equal 100 dB. From figure (4.18), we observe that Pd of the Bayesian CFAR detector decreases by a small value although the interference power is high but Pd of the OS-CFAR increases by a higher value than the previous detector. After that, we add a second interference in the reference cells. Figure (4.19) shows that Pd of the

OS-CFAR decreases significantly by comparison with the Bayesian CFAR detector where pd has approximately has the same value as in the case of one interference although the Pfa value of the two detectors is approximately = 10^{-3}. From all these results, we conclude that the Bayesian CFAR detector robust to strong interference.

4.7 Conclusion

In this chapter, we have analyzed the Bayesian CFAR detector in homogeneous and non homogeneous Pearson V distributed clutter and we compared the detection performance with other detectors; namely the CA-CFAR, GO-CFAR, SO-CFAR and OS-CFAR. Then we have presented the theoretical analysis of the Bayesian CFAR detector and we derived a new semi analytical expression of Pfa, which is different from the Pfa corresponding to Neyman-Pearson criterion. The results have shown that the Bayesian CFAR detector has the best performance compared with other detectors in homogeneous clutter. In non homogeneous clutter, we have added interferences in the reference cells, and we compared the detection performance with the OS-CFAR. The analysis showed that the performance of Bayesian CFAR detector did not degrade when the level of interferences increases. The Bayesian CFAR and OS-CFAR detectors were able to regulate the Pfa reasonably even for high level interferences.

Chapter 5

General Conclusions and Suggestions

Contents

Abstract

In this final chapter, we first briefly recall the main work of this thesis, and then we discuss our contributions including the main results. Finally, we list the possible perspectives and suggestions that can serve as extensions to this research work..

5.1 Summary of Work

Parameter Estimation is a very important step in radar system. Usually, this task is used to estimate sea clutter parameters as non-Gaussian and Compound clutter. This task is the critical step to design or develop maritime radar, so that it can detect with high performance small targets (very spiky) and adjust the false alarm rate under different situations (homogeneous and non-homogeneous environment). Firstly, an Iterative Maximum Likelihood has been proposed for high-resolution sea clutter consisting of a compound distribution with speckle and a texture following a Inverse Compound Gaussian distribution in absence of thermal noise. This method uses two different methods which are the Maximum Likelihood and moment's method, the last one is used as initial points. We found two expressions of estimators corresponding to the two parameters that are shape and scale of the CIG distribution for K iterations. We compared the IMLE with other estimators such as MoM, NIOM, [zLog(z)] and MLE. After simulation, the results have shown that the IMLE has the best performance compared with MOM, NIOM and [zlog(z)]. As for the MLE and IMLE, they gave similar estimation performance especially when the clutter is very spiky which is the most interesting case in radar detection but the IMLE requires lower computational time. So, the IMLE has the best performance estimation compared with other estimators because of its law computational time. Finally, in the context of detection, we proposed a Bayesian detector in Pearson V clutter in homogeneous and non-homogeneous environment which is different from CFAR detector and we compared its performance with other CFAR detector that are: CA-CFAR, SO-CFAR, GO-CFAR and OS-CFAR. We found new expressions of the Pfa which is different from the classical old one. After that, we proved that the Bayesian a detector has the CFAR property and Pd was assessed using Monte Carlo simulation. The results have shown that the proposed Bayesian detector has the best performance compared with CA-CFAR, SO-CFAR and GO-CFAR in homogenous clutter. In non-homogeneous clutter, we have added different interferences and we compared with the OS-CFAR. The results have shown that the Bayes detector is robust to strong interferences. We can then conclude the Bayesian detector has the best performance compared to other CFAR detectors in homogeneous and non-homogeneous Pearson V environment.

5.2 Perspective and Future Work

In the light of the various results obtained during this thesis, different research perspectives can be considered. The axes that should be considered as perspectives for future work can be summarized as follows::

- Use the IMLE to estimate the parameters of Compound Inverse Gaussian plus thermal noise. In this case, three parameters are to be estimated.
- Use the Bayesian approach in detection for Compound Gaussian clutter such as K,

Pareto and Generalized Pareto that have two parameters in homogeneous and non-homogeneous clutter.

Radar system is a very fast domain, several modern methods are figured out in estimation and detection methods, we hope this work has given an added value in the field of high-resolution sea clutter radar estimation and detection.

Bibliography

[1] C. Wolff, "Radar basics", Radartutorial. [Online]. Available: https://www.radartutorial.eu/index.en.html. [Accessed: 28-Nov-2021].

[2] H.M. Finn, R.S. Johnson, "Adaptive detection mode with threshold control as a function of spatially sampled clutter level estimates", RCA Review, 29, September 1968, pp. 414–463.

[3] P.P.Gandhi, S.A.Kassam:"Analysis of CFAR processors in non homogenous background", IEEE Trans. Aerosp. Electron. Syst.,1988, 24, (4), pp. 427–445

[4] H.Rohling: "Radar CFAR thresholding in clutter and multiple target situations", IEEE Trans. Aerosp. Electron. Syst., 1983, 19, pp. 608–621

[5] K. D. Ward, R. J. A. Tough, and S. Watts, "Sea clutter: scattering, the K distribution and radar performance", Stevenage, Herts, United Kingdom: Institution of Engineering and Technology, 2013.

[6] D.R.Iskander, A.M.Zoubir: "A method for estimating the parameters of the K distribution using higher order and fractional moments", IEEE Trans. Aerosp. Electron. Syst., 1999, 35, (4), pp. 1453– 1457,

[7] A.Belleri, A.Nehorai, J.Wang: "Maximum likelihood estimation for compound Gaussian clutter with inverse gamma texture", IEEE Trans. Aerosp. Electron. Syst., 2007, 43, (2), pp. 775– 779,

[8] D.Blacknell, R.J.A.Tough: "Parameter estimation of the K-distribution based on [zlog(z)]", IEE Proc. on Radar, Sonar and Navig., 2001, 148, (10), pp. 309– 312.

[9] A.Mezache, A.Bentoumi, M. Sahed: "Parameter estimation for compound-Gaussian clutter with inverse-Gaussian texture", IET Radar Sonar Navig., 2017, 11, (4), pp. 586–596, doi: https://doi/org/10.049/iet-rsn.2016.0208

[10] H. A. Meziani and F. Soltani, "Performance analysis of some CFAR detectors in homogeneous and non-homogeneous Pearson-distributed clutter", Signal Process., vol. 86, no. 8, pp. 2115–2122, Aug. 2006, doi: 10.1016/j.sigpro.2006.02.036.

[11] H. Rahman,"Fundamental principles of radar". Boca Raton: Taylor and Francis, 2019.

[12] N.Guidoum "Modélisation et Estimation des Paramètres d'un Fouillis Non-Gaussien", thèse de doctorat, Université Frères Mentouri Constantine 1, 2020-2021.

[13] M. A. Richards, J. Scheer, W. A. Holm, and W. L. Melvin, Eds., "Principles of modern radar". Raleigh, NC: SciTech Pub, 2010.

[14] M. Barkat, "Signal detection and estimation", Boston: Artech House, 2005.

[15] M. I. Skolnik, "Radar Handbook", New York: McGraw-Hill, 2008.

[16] S. Chen, "Principles of synthetic aperture radar imaging: a system simulation approach", Boca Raton: CRC Press/Taylor and amp; Francis Group, 2019.

[17] J. Bech, J. L. Chau, "Doppler radar observations: weather radar, wind Profiler, ionospheric radar, and other advanced applications", Rijeka: InTech, 2012.

[18] L.Rosenberg, S.Watts, "Radar Sea Clutter:Modeling and target detection", Satech Publiching, 2022.

[19] E.Ollila, D.Tyler, E Koivunen, V. et. al.: "Compound-Gaussian clutter modelling with an inverse Gaussian texture distribution", IEEE Signal Process. Lett., 2012, 19, (12), pp. 876– 879.

[20] P.L.Shui, L.X.Shi, Y.T.Huang: "Iterative Maximum likelihood and outlier-robust bipercentile estimation of parameters of compound-Gaussian clutter with inverse Gaussian texture", IEEE Signal Process. Lett., 2016, 23, (11), pp. 1572– 1576.

[21] A. Mezache, F.Soltani, M. et al.Sahed: "Model for non-Rayleigh clutter amplitudes using compound inverse Gaussian distribution: an Experimental analysis', IEEE Trans. Aerosp. Electron. Syst, 2015, 51, (1), pp. 142– 153.

[22] D. Schleher, "Radar detection in Weibull clutter", IEEE Transactions on Aerospace and Electronic Systems, vol. AES-12, no. 6, pp. 736–743, 1976.

[23] J.O.Berger, "Statistical Decision Theory and Bayesian Analysis", Springer New York, NY, 1985.

[24] G. V. Weinberg, S. D. Howard, and C. Tran, "Bayesian framework for detector development in Pareto distributed clutter", IET Radar Sonar Navig., vol. 13, no. 9, pp. 1548–1555, Sep. 2019, doi: 10.1049/iet-rsn.2018.5635.

[25] G. V.Weinberg,S. D. Howard, C.Tran: "A Bayesian-based CFAR detectorfor Pareto type II clutter". IEEE Int. Conf. on Radar, Brisbane, 2018.

[26] H. A. Meziani and F. Soltani, "Decentralized fuzzy CFAR detectors in homogeneous Pearson clutter background", Signal Process., vol. 91, no. 11, pp. 2530–2540, Nov. 2011, doi: 10.1016/j.sigpro.2011.05.006.

[27] H.A.Meziani "analyse des détecteurs adaptatifs CFAR dans un fouillis de distribution Pearson", thèse de doctorat, Université Frères Mentouri Constantine 1, 2020-2021.2008-2009.

[28] H. A. Meziani and F. Soltani, "Optimum second threshold for the CFAR binary integrator in Pearson-distributed clutter", Signal Image Video Process., vol. 6, no. 2, pp. 223–230, Jun. 2012, doi: 10.1007/s11760-010-0207-3.

[29] P. Tsakalides, F. Trinci, C.L. Nikias, "Performance assessment of CFAR processors in Pearson-distributed clutter, IEEE Transactions on Aerospace and Electronic Systems", vol. AES- 36, 4, October 2000, pp. 1377–1386.

[30] H.effreys: "An invariant form for the prior probability in estimation problems", Proc. R. Soc. Lond. A. Math. Phys. Sci., 1946, 186, pp. 453–461.